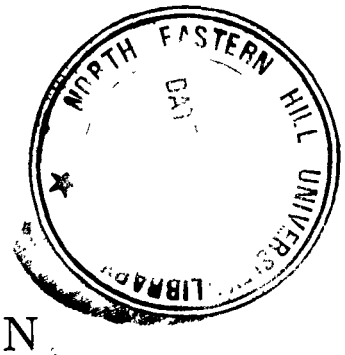

HYSTERESIS IN ANTI-FERROMAGNETIC RANDOM FIELD ISING MODEL

ABSTRACT OF Ph.D THESIS

BY

LOBISOR KURBAH

DEPARTMENT OF PHYSICS
NORTH EASTERN HILL UNIVERSITY
SHILLONG-793022

Physics

This thesis [1] concerns the study of hysteresis in anti-ferromagnetic random-field Ising model at zero temperature. The external field is cycled adiabatically between -∞ and ∞. Two different distributions of the random-field are considered, (i) a uniform distribution of width 2Δ centered at the origin, and (ii) a Gaussian distribution with average value zero and standard deviation σ. In each case the hysteresis loop is determined exactly in one dimension and compared with numerical simulations of the model. A very brief account of the broad context of the work, the model, the probabilistic method used to solve the model, and the end result is given below.

Hysteresis is a paradigm of non-equilibrium phenomena [2]. It occurs when a system is driven by a field that changes faster than the the system can cope with it. Feynman [3] in his book on statistical mechanics describes equilibrium as a state when all fast things have happened and slow things have not. What is fast and what is slow depends on the time scale of interest to us. Hot coffee in a cup may cool down to room temperature in a matter of minutes and then it may be considered to be in thermal equilibrium with its surroundings for hours. But over much longer period of weeks and months, the liquid in the cup is likely to evaporate into the air. In the context of hysteresis, the time period τ of the driving field serves as a reference. There is pronounced hysteresis if the relaxation time τ_{relax} of the system is larger than τ. The experimentalist controls τ i.e. the frequency of the driving field $\omega = 2\pi/\tau$, but τ_{relax} is fixed for a given material. By choosing $\tau > \tau_{relax}$, one can study systems close to equilibrium, i.e. hysteresis loops whose area tends to zero. However, several systems are never close to equilibrium. These are generally systems that contain quenched disorder. The quenched disorder creates a large number of metastable states that are separated from each other by large barriers [4]. The relaxation time (escape from a metastable state) diverges exponentially with the ratio of the barrier height to the thermal energy of the system. We may consider the system to be at zero temperature without compromising with the essential physics of the phenomenon. The distribution of barrier heights translates into a distribution of relaxation

times. A spectrum of diverging relaxation times means the presence of hysteresis even in the limit $\tau \to \infty$. The limit $\tau \to \infty$ is a theoretical limit. In the laboratory τ can not be longer than the time available for the experiment. Systems with quenched disorder tend to show significant hysteresis over the longest practical time scale. For modeling this behavior we take the limit $T \to 0$ before the limit $\omega \to 0$. This gives nonvanishing hysteresis in the limit $\omega \to 0$.

Sethna and his co-workers [5] have introduced the non-equilibrium random-field Ising model to study hysteresis in disordered ferromagnets at zero temperature and in the limit $\omega \to 0$. The disorder in their model is characterized by on-site random fields having a Gaussian distribution with average value zero and standard deviation σ. They employ the zero temperature Glauber dynamics of Ising spins in their model, i.e. a spin flips only if it lowers the energy of the system. It is an iterative dynamics. If a spin flips it changes the net field on its neighbors and may cause them to flip as well. This may result in an avalanche of spin flips. The dynamics is applied till each spin in the system is stable. The applied field h changes infinitely slowly as compared with the time (i.e. the number of iterations) taken by the system to reach a stable state. This is implemented in the model by holding h constant during an avalanche. This model has been studied extensively in the case of ferromagnetic interactions using mean field theory, renormalization group, and numerical simulations [5]. Exact solutions of the ferromagnetic model have been obtained for Ising spins on a Bethe lattice of coordination number z [6–8], and continuous spins in the mean field limit [9].

Hysteresis in the anti-ferromagnetic random field Ising model [10–13] has received relatively little attention as compared to its ferromagnetic counter part. Only an expression for the major loop has been obtained [11] in one dimension in the case when the quenched field has a uniform distribution of width Δ centered at the origin and $\Delta < |J|$ where J is the anti-ferromagnetic exchange interaction. The purpose of the present paper is to extend this result to $\Delta \geq |J|$. The results presented here also apply to a Gaussian distribution of the quenched random-field.

It may appear rather surprising at first sight that there should be any difficulty

in solving a one-dimensional Ising model at zero temperature. The difficulty arises primarily from the presence of quenched random fields. In general, problems with quenched disorder are difficult to analyze analytically. Problems with quenched disorder and anti-ferromagnetic interactions are more difficult. This is primarily due to two reasons. One, the relaxation process in the anti-ferromagnetic random-field Ising model depends on the order in which the spins are relaxed. Two, the energy landscape of the anti-ferromagnet has many more local minima than that of a ferromagnet.

The one-dimensional random-field Ising model is characterized by the Hamiltonian,

$$H = -J\sum_i s_i s_{i+1} - \sum_i h_i s_i - h_a \sum_i s_i. \tag{1}$$

Here $s_i = \pm 1$ is an Ising spin at site i ($i = 1, 2, 3, \ldots, N$), J is the nearest neighbor interaction ($J > 0$ for a ferromagnet and $J < 0$ for an anti-ferromagnet), h_i is a random-field drawn from a probability distribution $\phi(h_i)$, and h_a a uniform external field.

The dynamics of the model is the discrete-time single-spin-flip Glauber dynamics at zero temperature i.e. $s_i(t+1) =$ sign $f_i(t)$, where

$$f_i = J(s_{i-1} + s_{i+1}) + h_i + h_a \tag{2}$$

This means a spin flips only if it lowers its energy. It also assumes that if a spin-flip is allowed, it occurs at a rate which is much faster than the rate at which the magnetic field h_a is varied. Iterative application of the dynamics leads to a fixed point state of the system such that $s_i(t+1) = s_i(t)$ for each spin $s_i(t)$ in the system. The condition of adiabatic variation of the applied field is implemented by holding the applied field constant until a fixed point is reached. The fixed point is a local minimum of the energy (metastable state) of the system. Our aim is to find the magnetization $m(h_a)$ of each metastable state visited by the system as the applied field is cycled adiabatically from $h_a = -\infty$

to $h_a = \infty$. The magnetization along the upper half of the hysteresis loop is given by symmetry, $m^u(h_a) = -m(-h_a)$. We have $m(h_a) = 1 - 2P_\downarrow(h_a)$ where $P_\downarrow(h_a)$ is the probability that a randomly chosen site i is down (i.e. $s_i = -1$) at an applied field h_a. $P_\downarrow(h_a)$ is a function of $p_n(h_a)$, where

$$p_n(h_a) = \int_{-2(1-n)|J|-h_a}^{\infty} \phi(h_i) dh_i \ (n = 0, 1, 2) \tag{3}$$

We say that a site flips up under a p_n-process if n of its nearest neighbors are up when it flips up. In order to calculate $P_\downarrow(h_a)$ we make use of the screening property of a pair of adjacent down sites (doublet) that have remained unflipped in a monotonically increasing field from $-\infty$ to h_a. A doublet separates the chain into two parts that have evolved independently of each other. The doublet also provides a natural length in the analysis of the chain. This is not a fixed length but rather a variable length of a segment of chain that is free of doublets and lies between two doublets at an applied field h_a. The history of evolution of this segment may be analyzed independently of the rest of the chain. We denote the probability per site of finding a doublet on the chain by $P_{\downarrow\downarrow}(h_a)$, and find

$$P_{\downarrow\downarrow}(h_a) = \left[P_{\downarrow\downarrow}(1\downarrow|0\downarrow: h_a)\right]^2, \tag{4}$$

where

$$P_{\downarrow\downarrow}(1\downarrow|0\downarrow; h_a) = e^{-p_0(h_a)} - \left[e^{-p_1(h_a)} - \{1 - p_1(h_a)\}\right] - \sum_{n=3}^{\infty}(-1)^n T_n(h_a), \tag{5}$$

$$T_n(h_a) = \int_{-2|J|-h_a}^{-h_a} \phi(h_1) dh_1 \left[\prod_{m=3}^{n-1} \int_{h_{m-2}+2|J|}^{\infty} \phi(h_{m-1}) dh_{m-1}\right] \int_{h_{n-2}+2|J|}^{\infty} \tilde{\phi}(h_{n-1}) dh_{n-1}, \tag{6}$$

and

$$\tilde{\phi}(h) = [1 - e^{-p_0(-h-2|J|)}]\phi(h) \tag{7}$$

This is a generalization of a result derived in reference [11]. The result in reference [11] is valid in a special case when no $p_n(h_a)$ process can begin before all $p_{n-1}(h_a)$ processes have been completed everywhere on the chain.

In order to calculate the probability that a randomly chosen site i is down at an applied field h_a, we need to calculate the probability of a large number of related events concerning the history of spin flips at site i and its neighbors at sites $i-1$ and $i+1$. If site i is down at h_a, it may have never flipped from $h_a = -\infty$ to h_a, or it may have flipped two times. Its neighbors too may have flipped zero, one, or two times. The probability of flipping at a site depends on the state of its neighbors. If both neighbors are up, we may have to take into account which one flipped first. If a neighbor flipped under a p_1 process we have to take into account if the p_1 process pre-empted a p_0 process or not. Careful considerations of these issued show that we need to calculate the probability of 26 distinct processes. The final result is,

$$\begin{aligned} P_{\downarrow}(h_a) = P_{\downarrow\downarrow\downarrow}(h_a) + P_{\downarrow\downarrow\uparrow}(h_a) + P_{\uparrow\downarrow\downarrow}(h_a) + P_{\uparrow\downarrow\uparrow A}(h_a) + P_{\uparrow\downarrow\uparrow D}(h_a) \\ -P_{\uparrow\uparrow\uparrow M}(h_a) - P_{\uparrow\uparrow\uparrow N}(h_a) - P_{\uparrow\uparrow\uparrow 0}(h_a) - P_{\uparrow\uparrow\uparrow P}(h_a) \\ +P_{\uparrow\downarrow\uparrow Q}(h_a) + P_{\uparrow\downarrow\uparrow R}(h_a) + P_{\uparrow\downarrow\uparrow S}(h_a) + P_{\uparrow\downarrow\uparrow T}(h_a) \\ -P_{\uparrow\uparrow\uparrow U}(h_a) - P_{\uparrow\uparrow\uparrow V}(h_a) - P_{\uparrow\uparrow\uparrow W}(h_a) - P_{\uparrow\uparrow\uparrow X}(h_a), \end{aligned} \tag{8}$$

where,

$$P_{\downarrow\downarrow\downarrow}(h_a) = [1 - p_0(h_a)]P\downarrow\downarrow(h_a) \tag{9}$$

$$P_{\downarrow\downarrow\uparrow}(h_a) = P_{\uparrow\downarrow\downarrow}(h_a) = p_0(h_a)P_{\downarrow\downarrow}(h_a) \tag{10}$$

$$\begin{aligned} P_{\uparrow\downarrow\uparrow A}(h_a) &= \int_{-\infty}^{h_a} [P_{\downarrow\downarrow\uparrow}(h') + P_{\uparrow\downarrow\downarrow}(h')]\phi(-h' - 2|J|)dh' \\ &= \int_{-\infty}^{h_a} 2p_0(h')P_{\downarrow\downarrow}(h')\phi(-h' - 2|J|)dh' \end{aligned} \tag{11}$$

$$P_{\uparrow\downarrow\uparrow D}(h_a) = 2\int_{-\infty}^{h_a} dh'\tilde{\phi}(-h')p_0(h')P_{\downarrow\downarrow}(2\downarrow|3\downarrow;h') \tag{12}$$

$$\begin{aligned} P_{\uparrow\uparrow\uparrow M}(h_a) &= 2\int_{-\infty}^{h_a} dh'\tilde{\phi}(-h' + 2|J|) \\ \times \int_{h'-4|J|}^{h'-2|J|} dh''\phi(-h'' - 2|J|)&P_{\downarrow\downarrow}(3\downarrow|2\downarrow;h'') \end{aligned} \tag{13}$$

$$P_{\uparrow\uparrow\uparrow N}(h_a) = 2\int_{-\infty}^{h_a} dh'\tilde{\phi}(-h' + 2|J|)\int_{h'-4|J|}^{h'-2|J|} dh''\tilde{\phi}(-h'') \tag{14}$$

$$P_{\uparrow\uparrow\uparrow O}(h_a) = P_{\uparrow\downarrow\uparrow I}(h_a - 4|J|) \tag{15}$$

$$P_{\uparrow\uparrow\uparrow P}(h_a) = P_{\uparrow\downarrow\uparrow L}(h_a - 4|J|) \tag{16}$$

$$\begin{aligned} P_{\uparrow\downarrow\uparrow Q}(h_a) &= 2\int_{-\infty}^{h_a} dh'\phi(-h')P_{\downarrow\downarrow}(1\downarrow|2\downarrow;h') \\ \times \int_{h'-2|J|}^{h'} dh''\phi(-h'')P_{\downarrow\downarrow}(5\downarrow|4\downarrow;h'')&\int_{-h''}^{-h'+2|J|} dh'''\phi(-h''' - 2|J|) \end{aligned} \tag{17}$$

$$P_{\uparrow\downarrow\uparrow R}(h_a) = 2\int_{-\infty}^{h_a} dh'\tilde{\phi}(-h'+2|J|)\int_{h'-2|J|}^{h'} dh''\tilde{\phi}(-h''+2|J|) \times \int_{-h''}^{-h'+2|J|} dh'''\phi(-h'''-2|J|) \tag{18}$$

$$P_{\uparrow\downarrow\uparrow S}(h_a) = 2\int_{-\infty}^{h_a} dh'\tilde{\phi}(-h'+2|J|)\int_{h'-2|J|}^{h'} dh''\phi(-h'')P_{\downarrow\downarrow}(1\downarrow|2\downarrow;h'') \times \int_{-h''}^{-h'+2|J|} dh'''\phi(-h'''-2|J|) \tag{19}$$

$$P_{\uparrow\downarrow\uparrow T}(h_a) = 2\int_{-\infty}^{h_a} dh'\phi(-h')P_{\downarrow\downarrow}(1\downarrow|2\downarrow;h')\int_{h'-2|J|}^{h'} dh''\tilde{\phi}(-h''+2|J|) \times \int_{-h''}^{-h'+2|J|} dh'''\phi(-h'''-2|J|) \tag{20}$$

$$P_{\uparrow\uparrow\uparrow U}(h_a) = 2\int_{-\infty}^{h_a} dh'\phi(-h'+2|J|)\int_{h'-2|J|}^{h'} dh''\phi(-h'')P_{\downarrow\downarrow}(1\downarrow|2\downarrow;h'') \times \int_{h'-2|J|}^{h''} dh'''\phi(-h''')P_{\downarrow\downarrow}(5\downarrow|4\downarrow;h''') \tag{21}$$

$$P_{\uparrow\uparrow\uparrow V}(h_a) = 2\int_{-\infty}^{h_a} dh'\phi(-h'+2|J|)\int_{h'-2|J|}^{h'} dh''\tilde{\phi}(-h''+2|J|) \times \int_{h'-2|J|}^{h''} dh'''\tilde{\phi}(-h'''+2|J|) \tag{22}$$

$$P_{\uparrow\uparrow\uparrow W}(h_a) = 2\int_{-\infty}^{h_a} dh'\phi(-h'+2|J|)\int_{h'-2|J|}^{h'} dh''\tilde{\phi}(-h''+2|J|)$$
$$\times\int_{h'-2|J|}^{h''} dh'''\phi(-h''')P_{\downarrow\downarrow}(1\downarrow|2\downarrow;h''') \tag{23}$$

$$P_{\uparrow\uparrow\uparrow X}(h_a) = 2\int_{-\infty}^{h_a} dh'\phi(-h'+2|J|)\int_{h'-2|J|}^{h'} dh''\phi(-h'')P_{\downarrow\downarrow}(1\downarrow|2\downarrow;h'')$$
$$\times\int_{h'-2|J|}^{h''} dh'''\tilde{\phi}(-h'''+2|J|) \tag{24}$$

The calculation of $P_{\uparrow\uparrow\uparrow O}(h_a)$, and $P_{\uparrow\uparrow\uparrow P}(h_a)$ requires the following additional quantities,

$$P_{\uparrow\downarrow\uparrow B}(h_a) = 2\int_{-\infty}^{h_a}[P_{\downarrow\downarrow}(2\downarrow|3\downarrow:h') - \{1-p_0(h')\}]$$
$$P_{\downarrow\downarrow}(4\downarrow|3\downarrow:h')\phi(-h'-2|J|)dh' \tag{25}$$

$$P_{\uparrow\downarrow\uparrow C}(h_a) = P_{\uparrow\downarrow\uparrow A}(h_a) - P_{\uparrow\downarrow\uparrow B}(h_a) \tag{26}$$

$$P_{\uparrow\downarrow\uparrow E}(h_a) = 2\int_{-\infty}^{h_a} dh'\tilde{\phi}(-h')\,[P_{\downarrow\downarrow}(2\downarrow|3\downarrow;h') - \{1-p_0(h')\}] \tag{27}$$

$$P_{\uparrow\downarrow\uparrow F}(h_a) = P_{\uparrow\downarrow\uparrow D}(h_a) - P_{\uparrow\downarrow\uparrow E}(h_a) \tag{28}$$

$$P_{\uparrow\downarrow\uparrow G}(h_a) = \{1-p_0(h_a)\}[1-e^{-p_0(h_a)}]^2 \tag{29}$$

$$P_{\uparrow\downarrow\uparrow H}(h_a) = 2\{1 - p_0(h_a)\} \int_{-\infty}^{h_a} dh' P_{\downarrow\downarrow}(3\downarrow|2\downarrow; h')\phi(-2|J| - h') \times \int_{-\infty}^{h'} \tilde{\phi}(-h'')dh'' \tag{30}$$

$$P_{\uparrow\downarrow\uparrow I}(h_a) = P_{\uparrow\downarrow\uparrow C}(h_a) - P_{\uparrow\downarrow\uparrow G}(h_a) - P_{\uparrow\downarrow\uparrow H}(h_a) \tag{31}$$

$$P_{\uparrow\downarrow\uparrow J}(h_a) = [1 - p_0(h_a)] \left[\int_{-h_a}^{\infty} dh_3 \tilde{\phi}(h_3)\right]^2 \tag{32}$$

$$P_{\uparrow\downarrow\uparrow K}(h_a) = 2\{1 - p_0(h_a)\} \int_{-\infty}^{h_a} dh' \tilde{\phi}(-h') \times \int_{-\infty}^{h'} dh'' P_{\downarrow\downarrow}(3\downarrow|2\downarrow; h'')\phi(-h'' - 2|J|) \tag{33}$$

$$P_{\uparrow\downarrow\uparrow L}(h_a) = P_{\uparrow\downarrow\uparrow F}(h_a) - P_{\uparrow\downarrow\uparrow J}(h_a) - P_{\uparrow\downarrow\uparrow K}(h_a) \tag{34}$$

Numerical simulations have played a valuable role in our analysis. An exact analytic result has to be necessarily in agreement with the simulations within numerical errors but arguments based on conditional probabilities can be subtle and prone to errors. Therefore at each step of the analysis, we devised a simulation of the model to yield the probability of the event being calculated. Occasionally the two did not match in the first instance necessitating a rethink of the analysis and locating the error in the argument. Each theoretical expression contributing to the final result was tested by simulation of the model in the following cases: (i) bounded distribution with half-width $\Delta = 0.5|J|$; (ii) bounded distribution with $\Delta = 1.25|J|$; (iii) a Gaussian distribution with standard deviation $\sigma = .5|J|$. The average value of the random field is zero in all cases. As an illustration of the agreement between theory and simulation, figure (1) shows the hysteresis loop in

the case of the Gaussian distribution of the random field with $\sigma = 0.5|J|$. As the lower and the upper halves of the hysteresis loop are rather close to each other, we have reploted in figure (2) the upper and lower magnetizations relative to their average value. In both figures the data from the corresponding simulation is superimposed on the theoretical curve. The two are indistinguishable on the scale of the figure.

In conclusion we have obtained the zero-temperature hysteresis loop of a one dimensional anti-ferromagnetic random field Ising model in the case when the driving field varies from $-\infty$ to ∞ and back to $-\infty$ infinitely slowly. The problem is simple to state but difficult to solve. The end result for the hysteresis loop involves integrals that have to be evaluated numerically. We have shown that our theoretical results fit numerical simulations of the model quite well. However, several aspects of the problem still remain unsolved. For example we have obtained the hysteresis loop when the driving field takes the system from one saturated state ($h_a = -\infty$) to another ($h_a = \infty$). In this case we have a complete knowledge of the *a posteriori* distribution of the quenched field at different stages of evolution of the system. We are not in a position (so far) to obtain the hysteretic response of the system starting from an arbitrary initial state. It would be interesting to have an analytic solution of the problem in higher dimensions as well. Numerical simulations suggest that the anti-ferromagnetic hysteresis loops in higher dimensions have several plateaus for low values of Δ and σ as compared with $|J|$. Exact analytic solutions of problems with quenched disorder are difficult in statistical mechanics. One may even argue if they are worth the effort that has to be put in to try to obtain them. However exact solutions are intellectually satisfying and provide a framework for understanding a wide class of complex phenomena. We hope there will be more progress in this direction in the future.

Bibliography

[1] A paper based on the thesis and intended for publication is available on the cond-mat archive, arXiv:1104.0586; It also contains a more complete list of references.

[2] See for example, *The Science of Hysteresis*, edited by G Bertotti and I Mayergoyz, Academic Press, Amsterdam (2006).

[3] *Statistical Mechanics: A set of lectures* by R P Feynman, W A Benjamin, Inc., Reading, Massachusetts, USA (1972).

[4] *Spinglasses and Random Fields*, ed. A P Young, World Scientific, Singapore (1997).

[5] J P Sethna, K A Dahmen, S Kartha, J A Krumhansl, B W Roberts, and J D Shore, Phys Rev Lett 70, 3347 (1993); J P Sethna, K A Dahmen, and O. Percovic in [2] and references therein.

[6] P Shukla, Prog Theo Phys 96, 69-80 (1996); P Shukla, Physica A233, 235-241 (1996);P Shukla, Phys Rev E 62, 4725 (2000).

[7] D Dhar, P Shukla, and J P Sethna, J Phys A30, 5259 (1997).

[8] S Sabhapandit, P Shukla, and D Dhar, J Stat Phys 98, 103 (2000); S Sabhapandit, D Dhar, and P Shukla, Phys Rev Lett 88, 197202 (2002), P Shukla, Phys Rev E 63, 27102 (2001).

[9] P Shukla and R S Kharwanlang, Phys Rev E 81, 031106 (2010); P Shukla and R S Kharwanlang, Phys Rev E 83, 011121 (2011).

[10] P Shukla, Physica A233, 242-252 (1996).

[11] P Shukla, R Roy, and E Ray, Physica A 275, 380 (2000); P Shukla, R Roy, and E Ray, Physica A 276, 365 (2000).

[12] P Shukla, Int J Mod Phys B 17, 5583 (2003).

[13] J M Deutsch, A Dhar, and O Narayan, Phys Rev Lett 92, 227203 (2004).

Figures

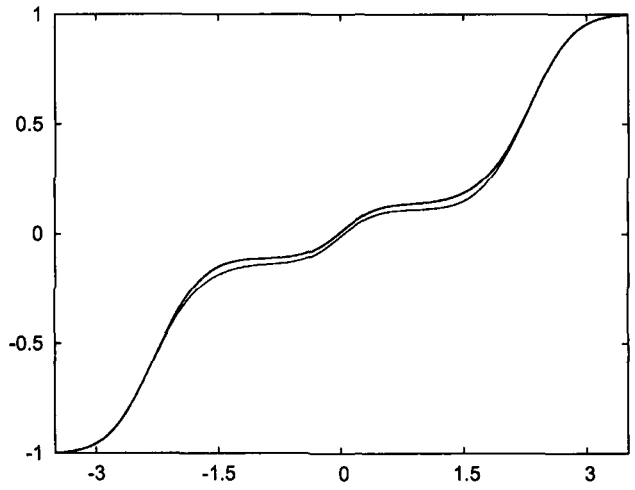

FIG. 1: Hysteresis loop for an anti-ferromagnetic random-field Ising model with $J = -1$ and a Gaussian distribution of the random field with $\sigma = 0.5$. Results of numerical simulation are superimposed on the theoretical expression.

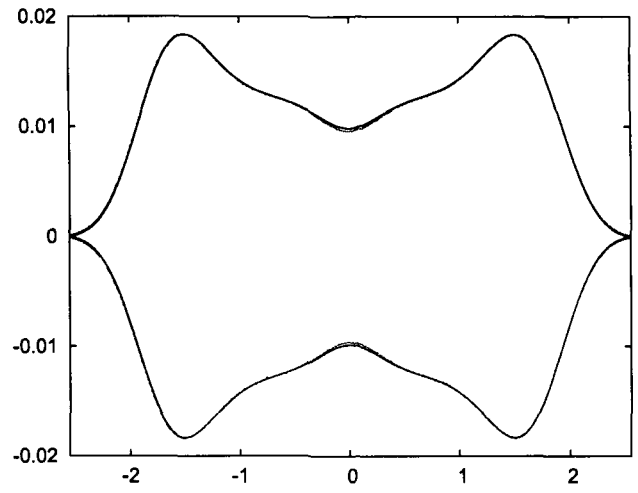

FIG. 2: Magnified theoretical and simulation hysteresis loops for $\sigma = 0.5$ where the magnetization along increasing and decreasing field is measured from the average of the magnetization on the lower and the upper half of the hysteresis loop in figure 1 at corresponding applied field.

Hysteresis in Anti-Ferromagnetic Random Field Ising Model

A THESIS SUBMITTED IN PARTIAL
FULFILMENT OF THE REQUIREMENT FOR
THE DEGREE OF

Doctor of Philosophy
in
Science

BY
LOBISOR KURBAH

DEPARTMENT OF PHYSICS
NORTH EASTERN HILL UNIVERSITY
SHILLONG-793022

Physics

The North Eastern Hill University

April 2011

I Lobisor Kurbah, hereby declare that the subject matter of this thesis is the record of work done by me, that the content of this thesis did not form basis of the award of any previous degree to me or to the best of my knowledge to anybody else. and that the thesis has not been submitted by me for any research degree in any other University/Institute.

This is being submitted to the North Eastern Hill University for the degree of Doctor of Philosophy in Physics.

26/04/11

(Lobisor Kurbah)

28/4/2011

Prof. P.N. Pandita

Head

Department of Physics

Prabodh Shukla

26/04/11

Prof. Prabodh Shukla

Supervisor

Acknowledgement

I am greatly indebted to my supervisor Prof. Prabodh Shukla for suggesting this problem and his invaluable guidance till the completion of this work. His patience, critical thinking and insistence on clarity has been most useful and inspiring. I would also take this opportunity to thank him for having faith in me even when situation are not encouraging.

I would like to thank the principal of St Edmund's college for granting me leave for two years without which it would not have been possible to complete this work. Also I would like to thank Regenal and all my colleages in the college for their encouragement.

I am thankful to all the faculty and the non-teaching staff of Physics Department for their help. Thanks are also due to Bahhep of the Computer Centre for his help in computer related problems.

I am grateful to the University Grant Commission for a fellowship under the faculty improvement programme.

Lastly I would like to mention my mama and my friend Shaili for all that they have done for me.

Place: Shillong

Date : 26th april 2011

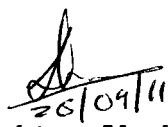

(Lobisor Kurbah)

Contents

List of figures

13. A doublet followed by a singlet (uniform random field, $\Delta \leq |J|$).

14. An up spin followed by a doublet (Gaussian random field).

15. A doublet followed by a doublet (Gaussian random field).

16. A singlet followed by a singlet (Gaussian random field).

17. A doublet followed by a singlet (Gaussian random field).

18. Theory and simulation for $P_{\downarrow\downarrow}(h_a)$ for a Gaussian distribution with $\sigma = 0.5$

19. Theory and simulation for $P_{\downarrow\downarrow}(h_a)$ for a uniform distribution with $\Delta = 1.25$

20. Theory and simulation for $P_{\downarrow\downarrow}(h_a)$ for a uniform distribution with $\Delta = 0.5$

21. Probability of $P_{\downarrow\downarrow\downarrow}(h_a)$ for a Gaussian distribution with $\sigma = 0.5$.

22. Probability of $P_{\downarrow\downarrow\downarrow}(h_a)$ for a uniform distribution with $\Delta = 1.25$.

23. Probability of $P_{\downarrow\downarrow\downarrow}(h_a)$ for a uniform distribution with $\Delta = 0.5$.

24. Probability of $P_{\uparrow\downarrow\downarrow}(h_a) + P_{\downarrow\downarrow\uparrow}(h_a)$ for a Gaussian distribution with $\sigma = 0.5$.

25. Probability of $P_{\uparrow\downarrow\downarrow}(h_a) + P_{\downarrow\downarrow\uparrow}(h_a)$ for a uniform distribution with $\Delta = 1.25$.

26. Probability of $P_{\uparrow\downarrow\downarrow}(h_a) + P_{\downarrow\downarrow\uparrow}(h_a)$ for a uniform distribution with $\Delta = 0.5$.

27. Theory and simulation of $P_{\uparrow\downarrow\uparrow A}(h_a)$ for a Gaussian distribution with $\sigma = 0.5$

28. Theory and simulation of $P_{\uparrow\downarrow\uparrow A}(h_a)$ for a uniform distribution with $\Delta = 1.25$

29. Theory and simulation of $P_{\uparrow\downarrow\uparrow A}(h_a)$ for a uniform distribution with $\Delta = 0.5$

30. Theory and simulation of $P_{\uparrow\downarrow\uparrow D}(h_a)$ for a Gaussian distribution with $\sigma = 0.5$

31. Theory and simulation of $P_{\uparrow\downarrow\uparrow D}(h_a)$ for a uniform distribution with $\Delta = 1.25$

32. Theory and simulation of $P_{\uparrow\downarrow\uparrow D}(h_a)$ for a uniform distribution with $\Delta = 0.5$

33. Probability of $P_{\uparrow\uparrow\uparrow M}(h_a)$ for a Gaussian distribution with $\sigma = 0.5$

34. Probability of $P_{\uparrow\uparrow\uparrow M}(h_a)$ for a uniform distribution with $\Delta = 1.25$

35. Probability of $P_{\uparrow\uparrow\uparrow M}(h_a)$ for a uniform distribution with $\Delta = 0.5$

36. Theory and simulation of $P_{\uparrow\uparrow\uparrow N}(h_a)$ for a Gaussian distribution with $\sigma = 0.5$

37. Theory and simulation of $P_{\uparrow\uparrow\uparrow N}(h_a)$ for a uniform distribution with $\Delta = 1.25$

38. Theory and simulation of $P_{\uparrow\uparrow\uparrow N}(h_a)$ for a uniform distribution with $\Delta = 0.5$

39. Theory and simulation of $P_{\uparrow\downarrow\uparrow Q}(h_a)$ for a Gaussian distribution with $\sigma = 0.5$

40. Theory and simulation of $P_{\uparrow\downarrow\uparrow Q}(h_a)$ for a uniform distribution with $\Delta = 1.25$

41. Theory and simulation of $P_{\uparrow\downarrow\uparrow Q}(h_a)$ for a uniform distribution with $\Delta = 0.5$

42. Probability of $P_{\uparrow\uparrow\uparrow U}(h_a)$ for a Gaussian distribution with $\sigma = 0.5$

43. Probability of $P_{\uparrow\uparrow\uparrow U}(h_a)$ for a uniform distribution with $\Delta = 1.25$

44. Probability of $P_{\uparrow\uparrow\uparrow U}(h_a)$ for a uniform distribution with $\Delta = 0.5$

45. Theory and simulation of $P_{\uparrow\uparrow\uparrow W}(h_a)$ for a Gaussian distribution with $\sigma = 0.5$

46. Theory and simulation of $P_{\uparrow\uparrow\uparrow W}(h_a)$ for a uniform distribution with $\Delta = 1.25$

47. Theory and simulation of $P_{\uparrow\uparrow\uparrow W}(h_a)$ for a uniform distribution with $\Delta = 0.5$

Preface

Statistical mechanics today is a pillar of theoretical physics. It started modestly in the form of kinetic theory of ideal gases in the 18th century but has made great strides in recent times. The task before statistical mechanics is to provide a manageable and useful description of an interacting system with a huge number of degrees of freedom. It is neither feasible nor useful to track each degree of freedom individually so one uses a small number of measurable variables like temperature, density, pressure etc. and treats these using probability theory. It is convenient to divide the thermodynamic systems into two categories: (i) equilibrium, and (ii) non-equilibrium. The assignment of a system to one of these categories is made on the basis of a characteristic time scale. The demarcation is not as sharp as we would like to think. For example, Feynman [1] in his book on statistical mechanics defines equilibrium as a state of the system when all fast things have happened and slow things have not. What is fast and what is slow depends on the time scale of interest to us. Hot coffee in a cup may cool down to room temperature in a matter of minutes and then it may be considered to be in thermal equilibrium with its surroundings for hours. But over much longer periods of weeks and months, the liquid in the cup is likely to evaporate into the air.

At present the statistical mechanics of systems in equilibrium is

far more developed than its counterpart for non-equilibrium systems. Its basic tools and methods are well established and well understood. A system in equilibrium at temperature T fluctuates between different states of energy E_i with the Boltzmann probability factor $\exp(-E_i/k_BT)$. The probability is normalized by summing the Boltzmann factor over all states. This sum is known as the partition function Z. The free-energy of the system is $F = -k_BT \ln Z$. Equilibrium state is a state of minimum free energy. Various measurable quantities can be obtained from the free-energy by differentiating it with respect to appropriate fields. Often it suffices to describe the measurable quantities and correlations in equilibrium systems by their average values. Phase transitions are an exception to this rule because they are marked by a diverging correlation length and anomalous fluctuations. However these problems have been addressed successfully by the renormalization group approach, and it is reasonable to say that the development of equilibrium statistical mechanics is nearly complete.

The development of equilibrium statistical mechanics has been greatly facilitated by exact solutions and numerical studies of simple models. For example, careful studies of Ising models in one, two, and three dimensions have contributed to the understanding of the scaling of thermodynamic functions in the critical region, and laid the foundation of the universality of critical behavior much before these ideas received full theoretical understanding based on

the renormalization group. Non-equilibrium statistical mechanics at present is in a developing state. A wide variety of models and phenomena are being studied. One hopes that results from such studies would lead to the understanding of general principles of systems far from equilibrium. The basic difference between equilibrium and non-equilibrium phenomena is the role of the relaxation dynamics in non-equilibrium phenomena. By relaxation we mean the dynamical process by which a system minimizes its free energy to attain thermal equilibrium. The character of the "fast things"! Equilibrium statistical mechanics need not go into the "what and how" of the fast things. It is content to assume that the fast things must have happened in such away as to endow the system with the necessary properties to be in equilibrium. For example, its occupation probability of different states must be governed by the Boltzmann factor. Other characterizations of equilibrium such as detailed balance, minimum free-energy, maximum entropy follow from the Boltzmann factor. In non-equilibrium statistical mechanics we have to study the details of the relaxation dynamics. This is a demanding task. The relaxation dynamics is system specific. Also, it would be neither useful nor practical to follow the time evolution of each individual degree of freedom. We should choose a small set of useful and measurable quantities in non-equilibrium and focus on the effect of the fast things on these quantities. Are these quantities just the non-equilibrium counterparts of temperature, density,

and pressure etc or there are better choices? It would take time to resolve these issues. The current activity seems to be focused on specific models and phenomena and what we may learn from these.

Hysteresis is a paradigm of non-equilibrium phenomena. If a system is driven by a cyclic field, and the time period of the field is shorter than the relaxation time of the system, then the system shows strong history-dependent non-equilibrium effects. The response of the system in increasing part of the cyclic field is different from that in the decreasing part. As the driving field makes a complete cycle the response of the system makes a hysteresis loop. The area of hysteresis loop determines the power consumed by the driving field. We are particularly interested in the effects of disorder on hysteresis. Disorder is unavoidable in a thermodynamic system. It can creep in the form of impurities and structural defects during the preparation of the system. It could be a small disorder e.g a tiny fraction of point defects in an otherwise perfect crystal, or a large disorder that is characteristic of liquids. Intuitively the meaning of small and large disorder is clear but there is no sharp division between the two. A more useful way to look at disorder is based on the relaxation dynamics of the system. If the disorder in the system is able to relax well over the experimental time scales, we called it annealed disorder. Annealed disorder is seen in very slowly cooled liquids and metals. If the disorder can not relax on experimental time scales, we call it quenched disorder. Quenched disorder remains

frozen in the system over practical time scales. Glasses, spinglass and other amorphous solid are example of quenched disorder. Annealed disorder is easier to treat analytically because the disorder degrees of freedom are dynamical variables that can be treated on equal footing with other degrees of freedom. Consider for example a mixture of magnetic ions with non-magnetic impurity atoms at a high temperature. If we allow the mixture to crystallize by cooling it slowly, the impurities and the magnetic ions will remain in thermal equilibrium with each other. The impurities are able to move. Therefore, to calculate the partition function of the system, we need to trace not only over the orientations of the spins of the magnetic ions but also over the positions of the impurity atoms. Quenched disorder on the other hand is difficult to treat analytically in equilibrium as well as non-equilibrium. In equilibrium, we have to calculate the partition function for a given disordered configuration of the system and then take the average of the logarithm of this partition function over different realizations of the disorder. In non-equilibrium too the analytic treatment of the dynamic degrees of freedom relaxing in a frozen background is more difficult. The frozen background creates a large number of metastable states in the system. These are separated from each other by high energy barriers. The energetics of the dynamics is primarily determined by the quenched disorder rather than thermal fluctuations. Although quenched disorder is more challenging to treat theoretically it is

creates a large number of metastable states in the system separated from each other by large barriers. The relaxation time (escape from a metastable state) in these materials diverges exponentially with the ratio of the barrier height to the thermal energy of the system. The distribution of barrier heights translates into a distribution of relaxation times. A spectrum of diverging relaxation times means that these materials show hysteresis even in the limit $\omega \rightarrow 0$.

Sethna and his co-workers [5–7] have introduced the non-equilibrium random-field Ising model to study hysteresis in disordered ferromagnets at zero temperature and in the limit $\omega \rightarrow 0$. The disorder in their model is characterized by on-site random fields having a Gaussian distribution with average value zero and standard deviation σ. They employ the zero temperature Glauber dynamics of Ising spins in their model, i.e. a spin flips only if it lowers the energy of the system. It is an iterative dynamics. If a spin flips it changes the net field on its neighbors and may cause them to flip as well. This may result in an avalanche of spin flips. The dynamics is applied till each spin in the system is stable. The applied field h changes infinitely slowly as compared with the time (i.e. the number of iterations) taken by the system to reach a stable state. This is implemented in the model by holding h constant during an avalanche. This model has been studied extensively in the case of ferromagnetic interactions using mean field theory, renormalization group, and numerical simulations. Exact solutions of

the model have also been obtained in one dimension [8, 9] and on a Bethe lattice of coordination number z [10]. Some exact results have also been obtained for continuous spin models in the mean field limit [11, 12]. There is comparatively little work in the case of anti-ferromagnetic interactions. This thesis is a step in this direction. We present an exact calculation of the zero-temperature anti-ferromagnetic hysteresis loop in the zero-frequency limit of the driving field in one dimension. The problem appears simple but the analysis is unexpectedly complicated. The outline of the thesis is as follows.

Section I provides an introduction to the problem studied in this thesis. Section II defines the model for a general distribution of the quenched random-field centered at the origin. We focus on two specific cases: a uniform bounded distribution of width 2Δ and a Gaussian distribution of standard deviation σ. In section III we present numerical results for the hysteresis loop in three representative cases: $\Delta = 0.5$, $\Delta = 1.25$ and $\sigma = 0.5$. Section IV presents analytical calculation of the hysteresis loop in the case of a uniform distribution of the random-field of width 2Δ, with $\Delta \leq |J|$. Section V, section VI, and section VII form the main body of the thesis. These extends the result obtained in section IV to an arbitrary distribution of the random-field. Section VIII contains concluding remarks.

I. Introduction

Hysteresis is a non-equilibrium effect commonly observed in systems subjected to a cyclic force [13]. It means that the response to a changing force depends on the history of the force. In particular, the response in increasing force is different from that in decreasing force. This is caused by the delay in responding to the force. Theoretically hysteresis should disappear if the force changes sufficiently slowly but this often corresponds to unrealistically long time periods such as the life span of an experimentalist. Several complex and disordered systems like permanent magnets show hysteresis over the longest practical time scales. Experience with spinglasses and other systems containing quenched disorder [2] has revealed that the free energy landscape of such systems comprises a large number of local minima (metastable states). The number of local minima is thermodynamically large i.e. of the order of the number of degrees of freedom of the system. The barriers between the local minima are also large compared with the thermal energy of the system. Consequently, in the absence of a driving field the system gets trapped in one of the local minima and is unable to explore the entire phase space over practical time scales. In this situation the thermal relaxation time of the system τ is much larger than the relaxation time of its constituent units (individual spin-flips) as well as the period $2\pi/\omega$ of the cyclic driving field. Therefore a useful approx-

imation is to assume τ to be infinite or equivalently the system to be at absolute zero temperature. This makes the dynamics of the system deterministic and more amenable to analytic solutions and simulations without compromising the essential physics of the problem. We take the limit $T \to 0$ before the limit $\omega \to 0$ to obtain nonvanishing hysteresis in the limit $\omega = 0$.

In an extensive and pioneering work Sethna et al [5–7] used the random-field Ising model [3] along with the Glauber dynamics [14] at zero temperature to study hysteresis in ferromagnets with quenched disorder. They analyzed their model using numerical simulations, mean field theory, Wilson's renormalization group [15], and compared it with experiments. Their model reproduces several experimentally observed features. These include familiar shapes of hysteresis loops, Barkhausen noise [16], and return point memory. Interestingly the model predicts the existence of a non-equilibrium critical point on each half of the hysteresis loop. This is based on a Gaussian distribution of the random-field with mean value zero and standard deviation σ that plays the role of a tuning parameter in the model. The model may be solved exactly in one dimension and on Bethe lattices of a general coordination number z [8–10]. Above a lower critical coordination number z [10, 17] there is a critical value σ_c such that for $\sigma < \sigma_c$, each half of the hysteresis loop has a first order jump in the magnetization at some applied field h. The size of the jump goes to zero as $\sigma \to \sigma_c$ from below. If h_c is the crit-

ical field at which the jump vanishes, $\{h_c, \sigma_c\}$ is a non-equilibrium critical point showing scaling of thermodynamic functions and universality of critical exponents in its vicinity. This is reminiscent of equilibrium critical phenomena and appears to have a fair amount of experimental support in the field of hysteresis as well. A generalization of the model [11, 12, 18, 19] to n-component ($n > 1$) classical spins shows the existence of critical points in the generalized model as well. The critical exponents of the generalized model are in the universality class of the random-field Ising model ($n = 1$) if the critical point occurs at a non-zero value of magnetization or the applied field. This is understandable because a non-zero value of magnetization or the applied field picks a unique direction in the system that effectively reduces its symmetry to that of an Ising model. This lends further support to the broad agreement between experiments and predictions of RFIM for hysteresis.

Hysteresis in the anti-ferromagnetic random field Ising model [20–23] has received relatively little attention as compared to its ferromagnetic counter part [5–7, 10, 17, 24–29]. This is partly due to the difficulty of obtaining analytic solutions in the anti-ferromagnetic case. For the ferromagnetic case, exact expressions for the major and minor hysteresis loops have been obtained in one dimension as well as on a Bethe lattice of coordination number z for a bounded as well as a Gaussian distribution of the quenched field [10, 22, 23]. The distribution of Barkhausen jumps (avalanches) has

also been obtained [17]. Several other aspects of the ferromagnetic model have been studied in the mean field theory as well as on periodic lattices [26–29]. In the anti-ferromagnetic case an expression for the major loop has been obtained [12] in one dimension in case the quenched field has a uniform distribution of width Δ centered at the origin and $\Delta < |J|$ where J is the anti-ferromagnetic exchange interaction. The purpose of the present paper is to extend this result to $\Delta \geq |J|$ as well. The results presented here are also applicable to unbounded distributions of the quenched random-field such as the Gaussian distribution.

It may appear rather surprising at first sight that there should be any difficulty in solving a one-dimensional Ising model at zero temperature. The difficulty arises primarily from the presence of quenched random fields. Problems with quenched disorder are difficult to analyze analytically. Besides this the spin-flip dynamics with anti-ferromagnetic interactions is more complicated than its ferromagnetic partner. Consider two spin systems of equal size and having the same realization of quenched field distribution. Let one system have ferromagnetic nearest neighbor interaction J and the other an anti-ferromagnetic interaction $-J$. In equilibrium, the ground states of the two systems on a bi-partite lattice are related to each other by symmetry. Evidently no such relation is available between non-equilibrium metastable states of the two systems. An applied field h_a increasing adiabatically from $h_a = -\infty$ to $h_a = \infty$

takes both systems from a stable state with all spins pointing down (i.e. aligned along $h_a = -\infty$) to all spins pointing up. Although the end points of the trajectory are the same for both systems but the magnetization paths are different. In particular the number of metastable states along the two paths are different. In the ferromagnetic case, spins tend to flip up in avalanches and do not flip down in increasing field. The anti-ferromagnetic dynamics is marked by the absence of avalanches. This is because a spin flipping up at an applied field h_a prevents its neighbors from flipping up at the same field. However, a spin flipping up at h_a occasionally causes its neighbor to flip down at h_a. This is a kind of a reverse avalanche in anti-ferromagnetic dynamics that involves only two spins including the spin that triggers the avalanche. The forward avalanches in the ferromagnetic case, and the reverse avalanches in the anti-ferromagnetic case provide a mechanism for irreversibility in the two models respectively and give rise to hysteresis. Due to the smaller size of reverse avalanches the area of anti-ferromagnetic hysteresis loop is much smaller than the area of ferromagnetic loop. Also the Barkhausen noise on the ferromagnetic hysteresis loop that is caused by large sporadic avalanches is nearly absent in the anti-ferromagnetic case.

The relative difficulty of analyzing anti-ferromagnetic dynamics comes from the fact that it is non-Abelian while the ferromagnetic dynamics is Abelian. This means as follows. Consider an unstable

system at an applied field h_a such that one or more spins are not aligned along the net field at their site. We relax the system till it is stable. Relaxing the system means checking each spin and flipping it if it is not aligned along the net field at its site. It is an iterative process because flipping a spin may reverse the sign of the net field at its nearest neighbors. We have to continue the relaxation process till each spin in the system is stable. A dynamics is called Abelian if the end result of the relaxation process does not depend on the order in which the spins are relaxed. If the result does depend on the order in which the spins are relaxed it is called non-Abelian. Consider two nearest neighbor spins which are both down but the net field at their sites is positive. If the interaction between the spins is ferromagnetic, the spins can be relaxed in any order and the end result would be that both spins are turned up. This is because turning a spin up makes the net field at its neighbor even more positive so that the neighbor also has to be turned up. This is not the case with anti-ferromagnetic interactions. Turning a spin up decreases the net field at its neighbor and it may decrease it below zero so that the neighbor no longer needs to be turned up when relaxed. Thus the end result may be one spin up and one down. Which one is up depends on which one was turned up first. The anti-ferromagnetic dynamics is therefore non-Abelian. As the stable state at the end of the relaxation process depends on the order in which the unstable spins are relaxed, we have to choose a protocol

for the order in which the unstable spins are relaxed. At every step, we choose to relax the most unstable spin in the system i.e. the one whose flipping would lower the energy of the system the most. Locating the most unstable spin at every step of the dynamics is what makes the anti-ferromagnetic model more tedious to analyze theoretically as well as numerically.

Although the aim of the present study is to find an analytic solution of a non-equilibrium problem with quenched disorder, we may mention some connection with experiments. Relaxation dynamics of any complex statistical system belongs to one of two broad categories: (i) where relaxation takes place by avalanches, and (ii) where it proceeds by single localized events. The ferromagnetic random-field Ising model belongs to the category of avalanches. It explains experimental effects such as the Barkhausen noise and the possibility of non-equilibrium critical points. The anti-ferromagnetic random-field Ising models belongs to the second category characterized by the absence of avalanches. Due to the absence of avalanches, we do not expect small changes in the applied field to cause large changes spanning across the system. In other words, we do not expect the response of the system to be critical at any value of the applied field. This rules out the existence of non-equilibrium critical points in anti-ferromagnets. Our calculation shows that the hysteresis loop of an anti-ferromagnet with relatively small quenched disorder (to be defined in the following) has a wasp-waisted shape

i.e. constricted in the middle. In the limit of very small disorder the wasp-waisted shape gradually transforms into two hysteresis loops joined by a long and narrow region of almost no hysteresis. For much larger disorder the familiar pot-belly shape of ferromagnetic loops is recovered. Thus the anti-ferromagnets can exhibit a wide variety of shapes of hysteresis loops and this feature of our model is in general conformity with experiments [30–34]. Anti-ferromagnetic hysteresis loops comprising three loops are also observed in experiments [35, 36]. This too is understandable if our one-dimensional model is extended to lattices with higher coordination number. The anti-ferromagnetic model may also apply to other systems that exhibit glassy dynamics [8, 37–40] characterized by a single localized events.

II. The Model

We consider non-equilibrium anti-ferromagnetic random-field Ising model in one dimension at zero temperature. At each site i $(i = 1, 2, 3, \ldots, N)$ of a linear lattice, there is an Ising spin $s_i = \pm 1$ which interacts with its nearest neighbors through an anti-ferromagnetic interaction J $(J < 0)$. A quenched random-field h_i as well as a uniform externally applied field h_a acts on s_i. The Hamiltonian of the system is,

$$H = -J \sum_i s_i s_{i+1} - \sum_i h_i s_i - h_a \sum_i s_i \tag{1}$$

We consider two distributions $\phi(h_i)$ of the random-field $\{h_i\}$:

(a) A uniform bounded distribution of width 2Δ centered at the origin,

$$\begin{aligned} \phi(h_i) &= \tfrac{1}{2\Delta} \text{ if } [-\Delta \leq h_i \leq \Delta] \\ &= 0, \text{ otherwise.} \end{aligned} \tag{2}$$

(b) A Gaussian distribution with average zero and standard deviation σ,

$$\phi(h_i) = \frac{1}{\sqrt{2\pi\sigma^2}}\, e^{-\frac{h_i^2}{2\sigma^2}}. \tag{3}$$

It is convenient to rewrite H in terms of the net field f_i acting on spin s_i,

$$H = -\sum_i f_i s_i; \; f_i = J(s_{i-1} + s_{i+1}) + h_i + h_a \tag{4}$$

The spins $\{s_i(t) = \pm 1\}$ obey discrete-time single-spin-flip Glauber dynamics at zero temperature i.e. $s_i(t+1) = \text{sign } f_i(t)$. This means a spin flips only if it lowers its energy. It also assumes that if a spin-flip is allowed, it occurs at a rate Γ which is much larger than the rate at which the magnetic field h_a is varied. Thus all flippable spins relax instantly and $s_i(t+1)$ has the same sign as the net local field $f_i(t)$ at its site.

$$s_i(t+1) = \text{sign } f_i(t) = \text{sign } [J\{s_{i-1}(t) + s_{i+1}(t)\} + h_i + h_a(t)] \tag{5}$$

Iterative application of the above dynamics leads to a fixed point state of the system such that $s_i(t+1) = s_i(t)$ for each spin $s_i(t)$ in the system. The condition of adiabatic variation of the applied field or equivalently the instant relaxation of spins mentioned previously is implemented by holding the applied field constant until a fixed point is reached. The fixed point value of $s_i(t)$ does not depend on t as $t \to \infty$. We may therefore denote it by s_i^*. The fixed point is a local minimum of the energy (metastable state) of the system. We characterize it by its magnetization $m(h_a)$ per spin,

$$m(h_a) = \frac{1}{N} \sum_i s_i^* \tag{6}$$

Our aim is to find the magnetization $m(h_a)$ of each metastable state visited by the system as the applied field is cycled adiabatically from $h_a = -\infty$ to $h_a = \infty$ and back to $h_a = -\infty$. We start with $h_a = -\infty$ when each spin is necessarily aligned along the applied field i.e. we have a fixed point with $m = -1$. Now we increase h_a slowly till some spin becomes unstable and needs to be flipped. We flip that spin and check its neighborhood if any more spins have to be flipped. If any of the neighbors are flipped, we check their neighbors if they need to be flipped. This process is continued till no more spin needs to be flipped i.e. we have a new fixed point. The applied field is held constant during the passage from the old fixed point to the new. This procedure is continued up to $h_a = +\infty$ when $m = 1$. The magnetization $m^u(h_a)$ on the return trajectory when h_a is slowly decreased from $h_a = +\infty$ to $h_a = -\infty$ can be obtained from $m(h_a)$ by a symmetry relation $m^u(h_a) = -m(-h_a)$. Therefore the calculation of the lower half of the hysteresis loop suffices to determine the entire hysteresis loop.

III. Simulations

Computer simulations of the preceding model play a useful role in guiding its analysis and checking the analytic results. Normally we used 10^3 spins on a linear lattice with periodic boundary conditions and used 10^3 independent realizations of the random field distribution to generate the data. The data was binned in 10^3 bins in the applicable range of the applied field and average over different realization of the field distribution. The simulation results shown in figures (1)-(6) and some of the figures in section VIII were obtained in this way. It took approximately four hours on our 3 GHz desktop to generate the data for each figure. When the estimated probability of an event was very small, say of the order of 10^{-6}, we performed the corresponding simulation on a larger system, say 10^6 spins, and a smaller number of independent runs, say 10^2. This was to optimize the accuracy of the data and the time taken to generate it. We set $J = -1$, and as mentioned previously we performed simulations for three cases: (i) $\Delta = 0.5$, (ii) $\Delta = 1.25$, and (iii) $\sigma = 0.5$. These values were chosen arbitrarily but represent three broad classes of the analytic results. The simulations fit our theoretical results (to be presented in the following) quite well as may be expected from an exact solution. Indeed the two are indistinguishable on the scale of the figures. The fact that simulations over a relatively small size of the system agree with the exact results is

due to the super-exponential decay of correlations in this system[39]. The agreement between theory and simulation also justifies (albeit post facto) the implicit assumption in our analysis that the system is self-averaging.

A. $\Delta = 0.5$

Figure (1) shows the hysteresis loop for $\Delta = 0.5$. We see that $m(h_a) = -1$ if $h_a \leq -2|J| - \Delta$, and $m(h_a) = 1$ if $h_a \geq 2|J| + \Delta$. The magnetization $m(h_a)$ rises from -1 to +1 in three steps. We call these steps ramp-I ($h_a = -2|J| - \Delta$ to $h_a = -2|J| + \Delta$); ramp-II ($h_a = -\Delta$ to $h_a = +\Delta$); and ramp-III ($h_a = 2|J| - \Delta$ to $h_a = 2|J| + \Delta$). The ramps are connected to each other by two plateaus; plateau-I ($h_a = -2|J| + \Delta$ to $h_a = -\Delta$); and plateau-II ($h_a = +\Delta$ to $h_a = 2|J| - \Delta$). On the plateaus, the magnetization remains constant even though the applied field continues to increase. Plateaus occur for $\Delta \leq |J|$ (small disorder), and simulations suggest that magnetization on the plateaus is independent of Δ. Numerically, the magnetization on the plateaus is approximately $m^I = -.135$ on plateau-I, and $m^{II} = .109$ on plateau-II. The qualitative shape of $m(h_a)$ is easy to understand. Due to the anti-ferromagnetic interaction between nearest neighbors, spins with both neighbors down are the first to turn up in an increasing applied field. Such spins turn up on ramp-I. Next are the spins with one neighbor up and one down which turn up

on ramp-II. Spins with both neighbors up require the largest applied field to turn up, and these turn up on ramp-III. For $\Delta \leq |J|$, the three ramps are well separated from each other. In other words, no spin with n up neighbors ($n = 1, 2$) can turn up in increasing h_a until all spins with $n - 1$ up neighbors have turned up. On each ramp, the sequence in which the spins turn up is determined by the distribution of the quenched random field. Spins with large positive quenched field turn up before spins with a lower quenched field. The quenched field lies in the range $-\Delta$ to $+\Delta$. Thus each ramp has a width 2Δ along the axis of the applied field. When a spin turns up on ramp-I, its nearest neighbors are placed in a category so that they cannot turn up before ramp-II. Similarly when a spin turns up on ramp-II, its nearest neighbor which is down cannot turn up before ramp-III. This is essentially the reason for the absence of avalanches in the anti-ferromagnetic RFIM. Occasionally on ramp-II and ramp-III, a spin turning up can cause its nearest neighbor which is already up to turn down. We may call this a reverse avalanche of size unity. There are no long avalanches as in the ferromagnetic model. If there were no reverse flips at all there would be no hysteresis in the model. The smallness of the reverse flips is the reason behind the smallness of the area of the hysteresis loop. In order to highlight the separation of the upper and lower halves of the hysteresis loop we have plotted in figure (2) the relative separation of the two halves relative to their average value. As the

majority of the spins turn up one at a time, the calculation of $m(h_a)$ becomes essentially a matter of sorting quenched random fields in decreasing order on each ramp. The difficulty arises from the fact that *a posteriori* distribution of random fields on unflipped spins that are next to a flipped spin is significantly different from the initial uniform distribution. The main problem is to calculate this *a posteriori* probability distribution of random fields on unflipped spin sites.

B. $\Delta = 1.25$

Figure (3) shows the hysteresis loop for $\Delta = 1.25$. We see that the three ramps comprising the hysteresis loop in figure (1) have lost their individual identity. If $\Delta > |J|$, a spin with one neighbor up can turn up on the lower hysteresis loop before all spins with both neighbors have turned up. This makes the analysis of the dynamics more complex. We shall take it up in Section V and Section VI. Figure (4) is a magnified version of figure (3). It shows the relative separation of the two halves from their average value at a given applied field.

C. $\sigma = 0.5$

Figure (5) shows the hysteresis loop for $\sigma = 0.5$ for a Gaussian distribution of the random field. The Gaussian distribution is an

unbounded distribution. Therefore we may not expect the hysteresis loop to comprise of sharp ramps and plateaus as in figure (1). However, notice the qualitative similarity between figure (5) for $\sigma = 0.5$ and figure (1) for $\Delta = 0.5$ *sans* the sharp edges in figure (1). In spite of this qualitative similarity, the analysis of the hysteresis loop has to proceed on the lines of the analysis of figure (3). Indeed the general analysis presented in Section V , VI and VII applies equally to a uniform distribution with $\Delta > |J|$ and a Gaussian distribution for any value of σ. Figure (6) is a magnified version of figure (5) showing the relative separation of the two halves of the hysteresis loop from their average value at a given applied field. In view of the smallness of the area of the anti-ferromagnetic hysteresis loop, the magnified loops are better suited to judge the fit between simulation and theory to be presented in the following.

IV. Bounded distribution of quenched field with $\Delta \leq |J|$

If $\Delta \leq |J|$ and the applied field h_a is increased adiabatically from $-\infty$ to ∞, the spins with both neighbors down flip up first (ramp-I). Next are those with one neighbor up and one down (ramp-II). The last category of spins to flip up are those with both neighbors up (ramp-III). The ramps are separated by plateau-I and plateau-II. The width of the plateaus along the applied field axis decreases with increasing Δ and goes to zero as $\Delta \to |J|$. Magnetization on ramp-I was determined in reference [20] by exploiting a similarity between this problem and the problem of random sequential adsorption(RSA) [41]. The rate equations of the RSA problem were used to determine $m(h_a)$ on ramp-I, but they could not determine $m(h_a)$ on ramp-II and ramp-III. A different approach was introduced in [21, 22] which determined magnetization on all three ramps for $\Delta \leq |J|$. We recall this approach briefly because it serves as the starting point for analyzing magnetization curves for $\Delta > |J|$ as well as for a Gaussian distribution of random-fields. The following subsections contain the main results obtained in references [21, 22] with some reworking of notation and formalism.

A. Ramp-I

The analytical results for the magnetization on ramp-I are conveniently expressed in terms of three quantities $p_0(h_a)$, $p_1(h_a)$, and $p_2(h_a)$. These are the probabilities that a spin which has quenched field h_i and which has respectively zero, one, or two nearest neighbors up can flip up at applied field h_a. Thus,

$$p_n(h_a) = \int_{-2(1-n)|J|-h_a}^{\infty} \phi(h_i) dh_i \ (n = 0, 1, 2) \tag{7}$$

As the applied field increases adiabatically from $h_a = -\infty$ to $h_a = \infty$, spins with both neighbors down begin to flip up at $h_a = -2|J| - \Delta$ and continue to flip up till $h_a = -2|J| + \Delta$ at which stage ramp-I is completed and there are no down spins whose neighbors are also down. The fraction of up spins on ramp-I at an arbitrary applied field h_a is given by,

$$P_{\uparrow}^{I}(h_a) = \frac{1}{2}[1 - e^{-2p_0(h_a)}], \tag{8}$$

The central object in the calculation of $P_{\uparrow}^{I}(h_a)$ is the probability (per site) of finding a pair of adjacent down spins on ramp-I at applied field h_a. We denote this object by the symbol $P_{\downarrow\downarrow}^{I}(h_a)$. It is calculated as follows. Imagine coloring all sites with $h_i + 2|J| + h_a \geq 0$ black, and all sites with $h_i + 2|J| + h_a < 0$ white. Consider two adjacent down spins A and B shown in Figure (7). The sites A and

B can be both white, both black, or mixed. Given that A is down, it is clear that the state of B can only be influenced by the evolution of the system to the right of B. Similarly, given that B is down, the state of A can only be influenced by the evolution of the system to the left of A. We shall refer to this as the principle of conditional independence [42]. It requires

$$P^I_{\downarrow\downarrow}(h_a) = P(A \downarrow | B \downarrow) P(B \downarrow | A \downarrow) \tag{9}$$

where $P(A \downarrow | B \downarrow)$ is the probability that spin at site A is down given that spin at B is down, and $P(B \downarrow | A \downarrow)$ is the probability that B is down given that A is down. We take up the calculation of $P(B \downarrow | A \downarrow)$. If B is a white site, $P(B \downarrow | A \downarrow) = 1$ because white sites have not been relaxed from their initial state. If B is a black site and the site to the right of B is a white site then $P(B \downarrow | A \downarrow) = 0$. In general $P(B \downarrow | A \downarrow)$ depends on the length of the string of black sites to the right of B. Suppose B is a black site, and there are $(n-1)$ additional black sites to the right of B. In this case, the probability P^n_B that B is down satisfies the following recursion relation,

$$P^n_B = \frac{1}{n} P^{n-2}_B + (1 - \frac{1}{n}) P^{n-1}_B \tag{10}$$

The rationale for the above recursion relation is as follows. Let the black site farthest from B on the right be labeled as the *n-th* site. Any of the n sites could flip first. The probability that the

n-th site flips first is therefore equal to $\frac{1}{n}$. If this happens, (*n*-1)-*th* site is prevented from flipping up on ramp-I. The probability that B is down is now reduced to the probability that the end point of a chain of (*n*-2) black sites is down i.e. P_B^{n-2}. This accounts for the first term in equation (10). The probability that *n-th* site is not the first site to flip up is equal to $(1 - \frac{1}{n})$. Given this situation, the probability that B is down is equal to the probability that the end of a string of (*n*-1) black sites is down. This accounts for the second term in equation (10). We can rewrite the recursion relation (10) as

$$(P_B^n - P_B^{n-1}) = -\frac{1}{n}[P_B^{n-1} - P_B^{n-2}] \tag{11}$$

It has the solution,

$$P_B^n = \sum_{m=0}^{n} \frac{(-1)^m}{m!} \tag{12}$$

Summing over various possible values of n with appropriate weight, we get

$$\begin{aligned} P(B\downarrow|A\downarrow) &= \sum_{n=0}^{\infty}\sum_{m=0}^{n} \frac{(-1)^m}{m!} p_0^n(1-p_0) \\ &= \sum_{m=0}^{\infty} \frac{(-1)^m}{m!}(1-p_0)\sum_{n=m}^{\infty} p_0^n \\ &= \sum_{m=0}^{\infty} \frac{(-p_0)^m}{m!} = e^{-p_0} \end{aligned} \tag{13}$$

In the above array of equations, p_0 stands for $p_0(h_a)$. Thus,

$$P^I_{\downarrow\downarrow} = e^{-2p_0(h_a)} \tag{14}$$

Let $P^I_{\downarrow}$ be the probability per site of finding a down spin and $P^I_{\downarrow\uparrow}$ the probability per site of finding a down spin which is followed by an up spin. Clearly,

$$P^I_{\downarrow} = P^I_{\downarrow\downarrow} + P^I_{\downarrow\uparrow} = 1 - P^I_{\uparrow} \tag{15}$$

Keeping in mind that on ramp-I an up spin must be preceded (as well as followed) by a down spin, we get $P^I_{\downarrow\uparrow} = P^I_{\uparrow}$. Thus,

$$P^I_{\uparrow} = 1 - P^I_{\downarrow\downarrow} - P^I_{\uparrow}$$

or,

$$P^I_{\uparrow} = \frac{1}{2}[1 - P^I_{\downarrow\downarrow}] = \frac{1}{2}[1 - e^{-2p_0(h_a)}] \tag{16}$$

The magnetization on ramp-I is given by

$$m^I(h) = 2P^I_{\uparrow}(h) - 1 = -e^{-2p_0(h_a)} \tag{17}$$

The exact value of the magnetization on plateau-I is equal to $-\frac{1}{e^2}$ which is approximately equal to -.135.

B. Plateau-I

Plateau-I contains down spins in singlets and doublets punctuated by up spins. Each spin in a doublet has one neighbor up and one down. Therefore the net field on it is simply the sum of the random field h_i on its site and the applied field h_a. It turns up when $h_i+h_a \geq 0$. The random field lies in the range $-\Delta < h_i < +\Delta$. Therefore an applied field smaller than $-\Delta$ is sufficiently negative to pin down all doublets. This accounts for the range $(-2|J|+\Delta) < h_a < -\Delta$ where the magnetization shows a plateau. In each doublet, the spin with the larger quenched field h_i flips up on ramp-II when $h_i + h_a \geq 0$. The spin with the smaller quenched field then becomes a singlet which does not flip up before ramp-III. Thus, in order to find the form of ramp-II, we need to find the *a posteriori* distribution of quenched random fields on the doublets.

Consider a doublet on plateau-I as shown in Figure (8). The doublet sites are denoted as 1 and 2, and the quenched random fields on these sites are h_1 and h_2. The *a posteriori* probability distributions of h_1 and h_2 will be identical by symmetry. These distributions $\tilde{\phi}(h_1)$ and $\tilde{\phi}(h_2)$ are determined by the relaxation process on ramp-I. If the doublet survives up to plateau-I it must exist on ramp-I. Consider ramp-I at an applied field h_a. Given that site-2 is down at this point, the probability that site-1 is also down is equal to $e^{-p_0(h)}$. Site-1 may be down because (i) it is a white site i.e. $h_1+2|J|+h_a \leq 0$

and therefore it could not turn up even if both its nearest neighbors were down, or (ii) it is a black site but blocked from turning up by its neighbor that has turned up before it. The probability that it is a white site is equal to $1 - p_0(h_a)$. Therefore the probability that it is a black site but down at h_a is equal to $e^{-p_0(h_a)} - \{1 - p_0(h_a)\}$. This means,

$$Prob(1 \downarrow |2 \downarrow; h_1 + 2|J| + h_a \geq 0) = \int_{-2|J|-h_a}^{\Delta} \tilde{\phi}(h_1) dh_1$$
$$= \left[e^{-p_0(h_a)} - \{1 - p_0(h_a)\}\right]. \quad (18)$$

$\tilde{\phi}(h_1)$ is obtained by taking the derivative of the above expression. We get,

$$\tilde{\phi}(h_1)dh_1 = [1 - e^{-p_0(-h_1-2|J|)}]\phi(h_1)dh_1 \quad (19)$$

Assuming $h_1 > h_2$, site-1 would turn up on ramp-II when $h_1 + h_a = 0$. The density of sites on ramp-II at this value of the applied field is given by,

$$\tilde{\phi}(-h_a)dh_a = [1 - e^{-p_0(h_a-2|J|)}]\phi(-h_a)dh_a = [1 - e^{-p_1(h_a)}]\phi(-h_a)dh_a \quad (20)$$

We now address an issue which is crucial for determining ramp-II correctly. This concerns two adjacent doublets as shown in Figure

(9). What is the probability per site of observing this object on ramp-I? A doublet has an important property. It separates the lattice into two parts (one on each side of the doublet) which have evolved uninfluenced by each other. Thus, we can separate Figure (9) into three parts as enclosed in the dashed boxes. Evolution inside each box has remained shielded from the outside. The evolution in the middle box requires that site 3 flips up before site 2 or site 4. The probability for this event is equal to $\frac{1}{3}$. Given that site 2 is down, the probability that site 1 is down is equal to $e^{-p_0(h_a)}$. Similarly, given that site 4 is down the probability that site 5 is down is equal to $e^{-p_0(h_a)}$. Thus the probability per site of observing two adjacent doublets on ramp-I at an applied field h_a is equal to $\frac{1}{3}e^{-2p_0(h_a)}$. Note that it is quite different from the square of the probability of finding a single doublet! Let h_1, h_2, h_3, h_4 and h_5 denote the quenched fields at sites 1, 2, 3, 4, and 5 respectively. We are interested in the case $h_2 > h_1$, and $h_4 > h_5$, and ask what are *a posteriori* distribution of fields $h_1, h_2, \ldots, h_5$ on ramp-II. Let the probability that $h_i (i = 1, \ldots, 5)$ lies in the range $[-h_a - dh_a, -h_a]$ on ramp-II be denoted by $\rho_i(-h_a)dh_a$. The distributions of h_1 and h_5 are given by,

$$\rho_1(-h_a) = \frac{\{1 - e^{-p_1(h_a)}\}}{e^{-p_0(h_a)}}\phi(-h_a) \tag{21}$$

$$\rho_5(-h_a) = \frac{\{1 - e^{-p_1(h_a)}\}}{e^{-p_0(h_a)}}\phi(-h_a) \tag{22}$$

Equation (21) is obtained as follows. If sites 1 and 2 are down on plateau-I, they must have been down all along ramp-I. Given that site 2 is down on ramp-I, the probability that site-1 is down is equal to $e^{-p_0(h_a)}$. This accounts for the denominator. The numerator gives the *a posteriori* probability distribution of the quenched field at site 1 on the lines of the preceding discussion with reference to figure (8). Equation (22) is written similarly. Note that the distributions $\rho_1(h_i)$ and $\rho_5(h_i)$ are each normalized to unity. Next we turn to the distributions of h_2, h_3, and h_4. As stated previously, $h_2 > h_1$ and $h_4 > h_5$ so we are looking at the case where h_2 and h_4 flip up on ramp-II. We may assume without loss of generality that $h_4 > h_2$. Let h_4 flips up on ramp-II at applied field h_a i.e. $h_4 + h_a = 0$. The probability for this is equal to $\phi(-h_a)p_1(h_a)\{1 - p_1(h_a)\}$; the three multiplicative factors giving respectively the probability that $h_4 = -h_a$, site 3 is up at h_a, and site 2 is down at h_a. Thus,

$$\rho_4(-h_a) = 6p_1(h_a)\{1 - p_1(h_a)\}\phi(-h_a) \tag{23}$$

The factor of 6 on the rhs arises as follows. At h_a on ramp-II site 2 will be down and sites 3 and 4 will be up at h_a given that at an earlier field $h_a - 2|J|$ on ramp-I site 3 had flipped up before 2 and 4 with probability $\frac{1}{3}$. The site flipping up on ramp-II may be to the left of the central site or to its right. This gives an additional factor of 2.

The distribution of h_2 is obtained similarly. We find,

$$\rho_2(-h_a) = 3p_1^2(h_a)\phi(-h_a) \tag{24}$$

C. Ramp-II

Ramp-II is determined by the combination of two terms. The dominant term is the increase in magnetization due to the decrease in the number of doublets. When a doublet disappears, it adds an extra up spin in the system which increases the magnetization. Occasionally, a disappearing doublet creates a string of three up spins. A triplet of up spins is unstable on ramp-II if $\Delta \leq |J|$ and therefore the central spin of the triplet flips down as soon as the triplet is created. This decreases the magnetization. In the following, we calculate the above two terms separately. Refer to figure (8) for calculating the first term. Let us assume $h_1 < h_2$. The *a posteriori* distribution of fields h_1 and h_2 in figure (8) are the same as $\rho_1(h_1)$ in figure (9). The probability that the doublet disappears at $h_2 + h_a = 0$ on ramp-II is given by

$$P_{\uparrow\uparrow}^{II} = 2e^{-2p_0(h_a)} \int_{-h_a}^{\infty} \rho_1(h_2)dh_2 \int_{-\infty}^{h_2} \rho_1(h_1)dh_1 \tag{25}$$

The factor $e^{-2p_0(h_a)}$ is the probability per site of finding a doublet at h_a before any of them have been relaxed. The factor 2 takes care of the fact that either h_1 or h_2 may be the larger field although

the expression is written on the assumption that site 2 flips up first. When a doublet disappears, a pair of adjacent up spins is created. This is the reason for the choice of the subscript on $P^{II}_{\uparrow\uparrow}$. The superscript indicates that the probability refers to ramp-II. We obtain,

$$P^{II}_{\uparrow\uparrow} = e^{-2p_0(h_a)} \left\{ \int_{-\infty}^{h_2} \rho_1(h_1) dh_1 \right\}^2 \Bigg|_{h_2=-h_a}^{h_2=\infty} \tag{26}$$

For $\Delta \leq |J|$, $p_0(h_a) = 1$ if $p_1(h_a) > 0$. Therefore,

$$P^{II}_{\uparrow\uparrow} = \frac{1}{e^2} - \left[(1 + e^{-1}) - \left\{ p_1(h_a) + e^{-p_1(h_a)} \right\} \right]^2 \tag{27}$$

We now calculate the fraction of (unstable) up triplets on ramp-II. Refer to figure (9) with the assumption that $h_2 < h_4$. An up triplet forms when $h_2 + h_a = 0$. The cumulative fraction of up triplets is given by,

$$P^{II}_{\uparrow\uparrow\uparrow} = \frac{1}{3} e^{-2p_0(h_a)} \int_{-h_a}^{\infty} \rho_2(h_2) dh_2 \int_{-\infty}^{h_2} \rho_1(h_1) dh_1 \int_{h_2}^{\infty} \tilde{\rho}_4(h_4) dh_4 \int_{-\infty}^{h_4} \rho_5(h_5) dh_5 \tag{28}$$

The two factors before the integrals give the probability per site of finding the object shown in Figure (9). These take into account the condition that $h_3 > h_4$. The next two integrals give the probability

that $h_2 + h_a = 0$ and $h_1 < h_2$. When h_2 is in the range $-h_a$ and $-h_a - \delta h_a$, h_4 can be anywhere in the range h_2 to ∞. Let $\rho_4(\tilde{h_4})$ be the density of h_4 in this range. Clearly,

$$\rho_2(h_2) = \int_{h_2}^{\infty} \tilde{\rho}_4(h_4) dh_4, \text{ or } \tilde{\rho}_4(h_i) = -\frac{d\rho_2(h_i)}{dh_i} \tag{29}$$

.

The integrals in equation (28) can be evaluated exactly for a uniform distribution. We get a non-zero contribution only if $p_1(h_a) > 0$. If $\Delta < |J|$ and $p_1(h_a) > 0$ then we must necessarily have $p_0(h_a) = 1$. Thus we get,

$$\begin{aligned} P^{II}_{\uparrow\uparrow\uparrow} = \frac{1}{3}\Bigg[& \frac{3}{2} + \frac{6}{e} - 6\left\{1 + \frac{1}{e}\right\} p_1(h_a) + 3p_1^2(h_a) \\ & + \left\{1 + \frac{1}{e}\right\}^2 p_1^3(h_a) - \frac{5}{4}\left\{1 + \frac{1}{e}\right\} p_1^4(h_a) + \frac{2}{5} p_1^5(h_a) \\ & - \left\{6\left(1 + \frac{1}{e}\right) - 6p_1(h_a) - 3\left(1 + \frac{1}{e}\right) p_1^2(h_a) + 2p_1^3(h_a)\right\} e^{-p_1(h_a)} \\ & + \left\{\frac{9}{2} + 3p_1(h_a)\right\} e^{-2p_1(h_a)}\Bigg] \end{aligned}$$

Putting the various terms together, the probability that a randomly chosen spin on the lattice is up on ramp-II is given by

$$P^{II}_{\uparrow}(h_a) = \frac{1}{2}[1 - e^{-2}] + P^{II}_{\uparrow\uparrow}(h_a) - P^{II}_{\uparrow\uparrow\uparrow}(h_a) \tag{30}$$

The magnetization on ramp-II is given by

$$m^{II}(h_a) = 2P_{\uparrow}^{II}(h_a) - 1 \tag{31}$$

The magnetization on plateau-II is equal to,

$$m^{II} = \left[\frac{27}{30} - \frac{7}{6}e^{-1} - \frac{8}{3}e^{-2}\right] = .109 \text{ (approximately)} \tag{32}$$

D. Plateau-II

Each down spin on plateau-II is a singlet. However, there are three different classes of singlets: the singlets formed on ramp-I; singlets formed on ramp-II by a vanishing doublet; and finally the singlets formed on ramp-II by the unstable central spin of an up triplet flipping down. The *a posteriori* distribution of random field is different for each class. Let ρ_a^{II}, ρ_b^{II}, and ρ_c^{II} denote the density of random fields in the three cases and P_a^{II}, P_b^{II}, and P_c^{II} be the probability of finding the corresponding singlet at applied field $h_a$on plateau-II.

$$P_x^{II}(h_a) = \int_{-h_a}^{\infty} \rho_x^{II}(h_i)dh_i, \text{ x=a, b, c} \tag{33}$$

It is useful to think of singlets in each class as being black or white on the ramp on which they are created. Suppose a singlet is created on ramp-I at applied field h_a'. It is created black if $h_i + 2|J| + h_a' \geq 0$,

and white if $h_i + 2|J| + h'_a < 0$ where h_i is the quenched random field at the singlet site. If a singlet is black at applied field h'_a then it is also black at fields greater than h'_a. A black singlet on ramp-I at h'_a will turn up on ramp-III at $h_a = h'_a + 4|J|$. Therefore if we know the fraction of black singlets on ramp-I we can calculate how they are destroyed on ramp-III.

The fraction of black singlets created on ramp-I is given by,

$$P_a^{II}(h'_a) = p_0(h'_a) - \frac{1}{2}\left[1 - e^{-2p_0(h'_a)}\right] - 2e^{-p_0(h'_a)}\left[e^{-p_0(h'_a)} - \{1 - p_0(h'_a)\}\right] \tag{34}$$

The explanation of the above equation is as follows. Imagine ordering the sites of the lattice in order of decreasing quenched field on the site. When all sites with $h_i + 2|J| + h'_a \geq 0$ have been relaxed, the fraction of the relaxed sites is equal to $p_0(h'_a)$ (the black sites). This fraction is made of the up sites (the second term on the right), black doublet sites (the last term), and the black singlets. Hence the equation for $P_1^{II}(h'_a)$. The last term is written as follows. In each doublet, there are two sites from which we can choose one. This accounts for the factor 2. The quantity in the square bracket gives the probability that the chosen site is black, and $e^{-p_0(h'_a)}$ is the probability that the other site can have any allowed value of the quenched field.

It is instructive to derive equation (34) by an alternate and more

direct method as well. We note that a pair of down spins on the chain has to be followed by a down spin or an up spin, i.e. $P_{\downarrow\downarrow} = P_{\downarrow\downarrow\downarrow} + P_{\downarrow\downarrow\uparrow}$. Similarly, $P_{\uparrow\downarrow\downarrow} + P_{\downarrow\downarrow\downarrow} = P_{\downarrow\downarrow}$. Thus,

$$\begin{aligned} P_{\uparrow\downarrow\downarrow}(h'_a) = P_{\downarrow\downarrow\uparrow}(h'_a) &= P_{\downarrow\downarrow}(h'_a) - P_{\downarrow\downarrow\downarrow}(h'_a) \\ &= e^{-2p_0(h'_a)} - \{1 - p_0(h'_a)\}e^{-2p_0(h'_a)} \\ &= p_0(h'_a)e^{-2p_0(h'_a)} \end{aligned} \tag{35}$$

We can obtain the fraction of singlets $P_{\uparrow\downarrow\uparrow}$ from $P_{\uparrow\downarrow\downarrow}$ and $P_{\downarrow\downarrow\uparrow}$ by calculating the probability that the down spin at either end flips up under a p_0 process.

$$\begin{aligned} P_{\uparrow\downarrow\uparrow}(h'_a) &= 2\int_{-\infty}^{h'_a} P_{\uparrow\downarrow\downarrow}(h''_a)\phi(-2|J| - h''_a)dh''_a \\ &= 2\int_0^{p_0(h'_a)} e^{-2p_0}p_0 dp_0 \\ &= \frac{1}{2}\left[1 - e^{-2p_0(h'_a)}\right] - p_0(h'_a)e^{-2p_0(h'_a)} \end{aligned} \tag{36}$$

The above expression gives the total fraction of singlets on ramp-I which include black ($h_i + 2|J| + h'_a \geq 0$) as well as white ($h_i + 2|J| + h'_a < 0$) singlets. The fraction of white singlets is given by,

$$P_{\uparrow\downarrow\uparrow}^{white}(h'_a) = \{1 - p_0(h'_a)\}[1 - e^{-p_0(h'_a)}]^2 \tag{37}$$

The first factor on the rhs gives the probability that the central site is white. Given that the central site is white, the probability that its neighbor is up is equal to $1 - e^{-p_0(h'_a)}$. The probability that both neighbors are up is equal to $[1 - e^{-p_0(h'_a)}]^2$. Thus,

$$P^{black}_{\uparrow\downarrow\uparrow}(h'_a) = P_{\uparrow\downarrow\uparrow}(h'_a) - P^{white}_{\uparrow\downarrow\uparrow}(h'_a)$$
$$= p_0(h'_a) - \frac{1}{2}\left[1 - e^{-2p_0(h'_a)}\right] - 2e^{-p_0(h'_a)}\left[e^{-p_0(h'_a)} - \{1 - p_0(h'_a)\}\right] \tag{38}$$

The fraction of black singlets on ramp-II ($h_i + h''_a \geq 0$) generated by vanishing doublets is given by,

$$P^{II}_b(h''_a) = \left[e^{-p_1(h''_a)} - \{1 - p_1(h''_a)\}\right]^2 \tag{39}$$

The above equation is easily understood. It is the probability that both sites of the doublet are black. If both sites of the doublet are black, the one with higher random field must flip up on ramp-II leaving us with a singlet on plateau-II which is black.

The fraction of black singlets created by unstable triplets requires the calculation of triplets. We have calculated the fraction of triplets as they are formed on ramp-II. What we need now is a similar but different calculation. The point can be understood with a reference to Figure (9). Recall that $h_3 \geq h_4 \geq h_2$. On ramp-II, we needed the fraction of triplets with $h_2 + h''_a \geq 0$, because the formation

of triplets is controlled by this threshold. The restoration of the triplets on ramp-III is controlled by the condition $h_3 - 2|J| + h_a \geq 0$. Keeping in mind that we want $h_1 \leq h_2$, and $h_5 \leq h_4$, the probability that $h_3 - 2|J| + h_a \geq 0$ is given by,

$$P_c^{II}(h_a) = 2\left[\int_{-h_a+2|J|}^{\infty} \phi(h_3)dh_3 \int_{-\infty}^{h_3} \rho_4(h_4)dh_4 \int_{-\infty}^{h_4} \rho_5(h_5)dh_5 \right.$$
$$\left. \int_{-\infty}^{h_4} \rho_2(h_2)dh_2 \int_{-\infty}^{h_2} \rho_1(h_1)dh_1\right]$$

Using $p_0(h_a) = 1$ and $p_1(h_a) = 1$ on plateau-II we get,

$$P_c^{II}(h_a) = -\left(1+\frac{2}{e}\right) + \left[\frac{1}{4}+\frac{2}{e}+\frac{4}{e^2}\right] p_2(h_a) - \frac{1}{2}\left[1+\frac{5}{e}+\frac{4}{e^2}\right] p_2^2(h_a)$$
$$+\frac{1}{3}\left[\frac{3}{2}+\frac{4}{e}+\frac{1}{e^2}\right] p_2^3(h_a) - \frac{1}{4}\left[1+\frac{1}{e}\right] p_2^4(h_a) + \frac{1}{20}p_2^5(h_a) + \left[1+\frac{2}{e}\right] e^{-p_2(h_a)}$$
$$-\frac{2}{e}p_2(h_a)e^{-p_2(h_a)} + p_2^2(h_a)e^{-p_2(h_a)} + \frac{1}{2}\left[1-e^{-2p_2(h_a)}\right] \quad (40)$$

E. Ramp-III

The rise of magnetization on ramp-III is due to singlet sites turning up in increasing field. At the start of ramp-III there are three categories of singlets present on plateau-II, and we have classified each of them conveniently into black and white singlets. The fraction of singlets on plateau-II that turn up at h_a on ramp-III is given by the fraction of black singlets in each of the three categories:

$$P^{III}(h_a) = P_a^{III}(h_a) + P_b^{III}(h_a) + P_c^{III}(h_a) \qquad (41)$$

However the calculation of magnetization on ramp-III turns out to be a bit more complicated. There is a new twist. Frequently when an original singlet site on plateau-II turns up on ramp-III its nearest neighbor turns down. We call this the creation of a new singlet on ramp-III. The newly created singlet site would turn up at a larger applied field on ramp-III. We shall call this event the destruction of the newly created singlet. We have to calculate the newly created singlets and their destruction before the magnetization on ramp-III may be obtained. It should be noted that this means that some sites flip three times in the course of a monotonic increase of applied field from $-\infty$ to ∞. However, no site flips more than three times.

When does a vanishing singlet on ramp-III create a new singlet on an adjacent site? Consider the singlet at site 3 in figure 10. Suppose site 3 flips up at h_a, i.e. $h_3 - 2|J| + h_a = 0$. Now the net field on site 2 is equal to $h_2 + h_a$. This is necessarily positive because $h_2 + 2|J| - h_3 \geq 0$ if $\Delta \leq |J|$. Thus site 2 would stay up after site 3 flips up. Consider site 4. After site 3 has turned up the net field at site 4 is equal to $h_4 - 2|J| + h_a$. Thus site 4 will turn down if $h_4 < h_3$. Site 3 will stay up even if site 4 turns down because $h_3 + h_a > 0$. These considerations can be put in the form of two guiding rules. When a singlet turns up on ramp-III, (i) its nearest neighbor stays

up if the next nearest neighbor is down, and $\Delta \leq |J|$, (ii) its nearest neighbor turns down if it has less quenched field than the singlet and the next nearest neighbor is up. Detailed considerations show that only the singlets created on ramp-I fall under the purview of these rules. Therefore we focus on the singlets present on plateau-I. Specifically we focus on the configurations shown in figure (11) and figure (12). In each of these figures a new singlet is created on site 3 when the singlet on site 2 is destroyed. The two figures make different contributions because of the role played by the next nearest neighbor of the singlet on the side of the newly created singlet.

The *a posteriori* distribution of the quenched field at site 2 is given by

$$\tilde{\tilde{\phi}}(h_2) = \left[1 - e^{-p_2(-h_2+2|J|)}\right] \phi(h_2) \tag{42}$$

The contributions of figure (11) to the fraction of newly created singlets when all sites with $h_i - 2|J| + h_a \geq 0$ have been relaxed on ramp-III is given by,

$$\begin{aligned} P_d^{III}(h_a) &= 2 \int_{-h_a+2|J|}^{\infty} \tilde{\tilde{\phi}}(h_2) dh_2 \int_{-\infty}^{h_2} \phi(h_3) dh_3 \int_{h_2}^{\infty} \tilde{\tilde{\phi}}(h_4) dh_4 \\ &= \frac{3}{2} - 2p_2(1-p_2) - \frac{2}{3}p_2^3 - 2(1 - p_2 + p_2^2)e^{-p_2} + \frac{1}{2}(1-2p_2)e^{-2p_2} \ . \end{aligned} \tag{43}$$

In the above and the following equations $p_2 \equiv p_2(h_a)$. Similarly

the contribution of figure (12) is,

$$
\begin{aligned}
P_e^{III}(h_a) &= \int_{-h_a+2|J|}^{\infty} \tilde{\tilde{\phi}}(h_2)dh_2 \int_{-\infty}^{h_2} \phi(h_3)dh_3 \int_{-\infty}^{h_3} \phi(h_4)dh4 \int_{-\infty}^{h_4} \tilde{\tilde{\phi}}(h_5)dh_5 \\
&= -\left(\frac{1}{3}+3e^{-1}\right)+\left(\frac{1}{3}+5e^{-1}\right)p_2-\left(\frac{1}{2}+2e^{-1}\right)p_2^2+\frac{1}{3}\left(1+e^{-1}\right)p_2^3 \\
&\quad -\frac{1}{12}p_2^4+\left\{\left(\frac{4}{3}+3e^{-1}\right)-\left(1+2e^{-1}\right)p_2+e^{-1}p_2^2-\frac{1}{3}p_2^3\right\}e^{-p_2}-e^{-2p_2}
\end{aligned}
\tag{44}
$$

In calculating the total fraction of newly created singlets, we have to multiply the contribution of figure (12) by 2 because an equal contribution is made by a configuration in which the doublet is to the left of the vanishing singlet.

The destruction of newly created singlets on ramp-III can be analyzed in a similar manner as their creation. The probability that site 3 flips for the third time in figure (11) is given by,

$$
\begin{aligned}
P_f^{III}(h_a) &= 2\int_{-h_a+2|J|}^{\infty} \phi(h_3)dh_3 \int_{h_3}^{\infty} \tilde{\tilde{\phi}}(h_2)dh_2 \int_{h_3}^{\infty} \tilde{\tilde{\phi}}(h_4)dh_4 \\
&= \frac{1}{2}\left[1-e^{-2p_2}\right]-2p_2e^{-p_2}+p_2(1-p_2)+\frac{1}{3}p_2^3
\end{aligned}
\tag{45}
$$

Similarly, the contribution to destruction of newly created singlet in figure (12) and another similar figure in which the doublet is to

the left of the singlet is given by,

$$P_g^{III}(h_a) = 2\int_{-h_a+2|J|}^{\infty} \phi(h_3)dh_3 \int_{h_3}^{\infty} \tilde{\tilde{\phi}}(h_2)dh_2 \int_{-\infty}^{h_3} \phi(h_4)dh4 \int_{-\infty}^{h_4} \tilde{\tilde{\phi}}(h_5)dh_5$$
$$= 2e^{-1} - \left(1+4e^{-1}\right)p_2 + \left(\frac{3}{2}+3e^{-1}\right)p_2^2 - \left(1+\frac{2}{3}e^{-1}\right)p_2^3 + \frac{1}{4}p_2^4$$
$$- \left\{\left(1+2e^{-1}\right) - 2\left(1+e^{-1}\right)p_2 + p_2^2\right\}e^{-p_2} + e^{-2p_2} \tag{46}$$

Putting all the terms together, the probability that a randomly chosen site on ramp-III is up is given by,

$$P_{\uparrow}^{III}(h_a) = P_{\uparrow}^{II}(h_a) + P_a^{III}(h_a) + P_b^{III}(h_a) + P_c^{III}(h_a)$$
$$-P_d^{III}(h_a) - P_e^{III}(h_a) + P_f^{III}(h_a) + P_g^{III}(h_a) \tag{47}$$

The magnetization in increasing field h_a is given by

$$m(h_a) = 2P_{\uparrow}^{III}(h_a) - 1 \tag{48}$$

The magnetization m_R on the return trajectory in decreasing field may be obtained by symmetry $m_R(h_a) = -m(-h_a)$. These results has been superimposed on the corresponding simulation data in figure (1) and figure (2). The simulation results for the return hysteresis loop were obtained independently without using the symmetry.

V. Unbounded distribution of quenched field

It is convenient to introduce the following nomenclature. We say that a site flips up under a p_0-process if none of its two nearest neighbors are up when it flips up. It is said to flip up under a p_1-process if it flips up when one of its neighbors is up and the other is down. Similarly, a site flipping up under a p_2-process has both its neighbors up at the time it flips up. The simplifying feature of the analysis for $\Delta \leq |J|$ is that a p_n-process ($n = 1, 2$) can not take place anywhere on the chain unless all p_{n-1} processes have been exhausted. In other words a new ramp can not begin before the previous ramp is completed. This feature is lost if $\Delta > |J|$ (or if the distribution is Gaussian) because a p_1 or a p_2 process can occur on the chain even if p_0-processes have not been exhausted (i.e. there remain strings of three down spins on the chain). The fact that p_0, p_1, and p_2 processes can run concurrently makes the calculation of *a posteriori* distribution of quenched fields at down sites more complicated than encountered in the preceding section.

Our first task is to calculate the probability of occurrence of a doublet in the chain. A doublet is a pair of adjacent down spins that have remained down in a monotonically increasing field from $-\infty$ to h_a. The significance of a doublet lies in its screening property. It separates the chain into two parts that have evolved independently of each other. The doublet also provides a natural length in the

analysis of the chain. This is not a fixed length but rather a variable length of a segment of chain that is free of doublets and lies between two doublets at an applied field h_a. The history of evolution of this segment may be analyzed independently of the rest of the chain. Let us focus on one end of such a segment. We label the sites $0, 1, 2, 3, \ldots, n$ starting from the left end of the segment. Our immediate object is to calculate the probability (per site of the chain) that site-0 and site-1 form a doublet at h_a. This is equal to $P^2_{\downarrow\downarrow}(1 \downarrow | 0 \downarrow; h_a)$ where $P_{\downarrow\downarrow}(1 \downarrow | 0 \downarrow; h_a)$ is the conditional probability that site-1 is down given that site-0 is down. We proved in section IV that $P_{\downarrow\downarrow}(1 \downarrow | 0 \downarrow; h_a) = e^{-p_0(h_a)}$ if only p_0-processes are allowed. This is an exact result on ramp-I for $\Delta \leq |J|$ and we take it as the leading term of the exact result for $\Delta > |J|$ or for an unbounded distribution such as the Gaussian distribution. The main effect of $\Delta < |J|$ is that if one of two adjacent sites say site-1 and site-2 ($h_1 + 2|J| + h_a \geq 0$ and $h_2 + 2|J| + h_a \geq 0$) flips up under a p_0-process then it prevents the other from doing the same. As long as $|h_1 - h_2| < 2|J|$ the same effect will be obtained at site-1 and site-2 for other distributions of the quenched field. In any particular realization of the quenched field distribution, the occurrence of a large connected cluster of sites with $h_{i+1} - h_i \geq 2|J|$ is rare. Therefore the case $\Delta < |J|$ serves as a good starting point for the exact result. Thus,

$$P_{\downarrow\downarrow}(1\downarrow|0\downarrow;h_a) = e^{-p_0(h_a)} \qquad \{\text{ leading term }\} \qquad (49)$$

Our approach is to add correction terms to the leading term to make it an exact result. The correction terms are functions of $p_1(h_a)$. No correction to the leading term is required if $p_1(h_a) = 0$. For $p_1(h_a) > 0$, the corrections may be divided into two categories. The first category is the one in which a doublet created by a p_0-process is subsequently destroyed by a p_1-process. This is similar to the fate of doublets on ramp-II for $\Delta \leq |J|$ and we get,

$$P_{\downarrow\downarrow}(1\downarrow|0\downarrow;h_a) = e^{-p_0(h_a)} - \left[e^{-p_1(h_a)} - \{1 - p_1(h_a)\}\right]$$
$$\{\text{ first order correction }\} \qquad (50)$$

The second category of correction involves events where a p_1-process pre-empts a p_0-process. These events are a signature of $\Delta > |J|$ and do not exist if $\Delta \leq |J|$. We illustrate this by a simple example. Suppose for a particular realization of the distribution of quenched fields $h_1, h_2, h_3, h_4 \ldots$, site-1, site-2, site-3 are black, site-4 is white, and $h_3 > h_2 > h_1$. If $\Delta < |J|$, site-3 will flip up first, block site-2 from flipping next, and therefore site-1 will flip up last. This will result in the absence of doublet at site-0 and site-1. Now consider $\Delta > |J|$ so that it is possible to have $h_2 > h_1 + 2|J|$ but

$h_1 + h_a < 0$. In this scenario site-3 will flip up first, then site-2, and site-1 will remain down giving us a doublet at site-0 and site-1 that was not allowed if $\Delta < |J|$. The probability of this new doublet created by a p_1-process pre-emptying a p_0-process is given by,

$$T_3(h_a) = \int_{-2|J|-h_a}^{-h_a} \phi(h_1)dh_1 \int_{h_1+2|J|}^{\infty} \tilde{\phi}(h_2)dh_2 \qquad (51)$$

Here $\tilde{\phi}(h_2)$ is given by equation (19) of section IV. This is because equation (19) of section IV gives the *a posteriori* distribution of the quenched field on a black site next to a site that has flipped up by a p_0-process. In our example site-2 is a black site next to site-3 that has flipped up by a p_0-process. $T_3(h_a)$ term is the leading term in the category of correction terms that arise because a p_1-process has pre-empted a p_0-process.

$$P_{\downarrow\downarrow}(1\downarrow|0\downarrow;h_a) = e^{-p_0(h_a)} - \left[e^{-p_1(h_a)} - \{1 - p_1(h_a)\}\right] + T_3(h_a)$$
$$\{ \text{ second order correction } \} \qquad (52)$$

The next correction comes from a cluster of adjacent spins that flip up as follows. Site-4 flips up under a p_0-process ($h_4 + 2|J| + h_a \geq 0$), site-3 flips next under a p_1-process ($h_3 > h_2 + 2|J|$), site-2 also flips under a p_1-process ($h_2 > h_1 + 2|J|$) after site-3 has flipped up, and site-1 remains down ($h_1 + h_a < 0, h_1 + 2|J| + h_a \geq 0$). The contribution from this event is,

$$T_4(h_a) = -\int_{-2|J|-h_a}^{-h_a} \phi(h_1)dh_1 \int_{h_1+2|J|}^{\infty} \phi(h_2)dh_2 \int_{h_2+2|J|}^{\infty} \tilde{\phi}(h_3)dh_3 \tag{53}$$

Notice that $T_3(h_a)$ is positive and $T_4(h_a)$ is negative. $T_3(h_a)$ is positive because it produces a doublet (at site-0 and site-1) where it did not exist under the p_0-process alone. $T_4(h_a)$ is negative for the following reason. T_4-process and p_0-process is mutually exclusive and since both contribute to a doublet then they must be added separately avoiding double counting. Thus the leading term in equation (49) under p_0-process alone is an overestimate and has to be reduced by an amount $T_4(h_a)$. However, T_4-process also gives rise to a doublet. Hence an amount equal to the one subtracted from the leading term has to be added to it resulting in zero correction to the leading term. Now consider the first correction shown in equation (50). This is an underestimate because it comes from the destruction of overestimated doublets in the leading term. It can be corrected by adding $T_4(h_a)$. The correct result at the present level of accuracy is,

$$P_{\downarrow\downarrow}(1\downarrow|0\downarrow;h_a) = e^{-p_0(h_a)} - \left[e^{-p_1(h_a)} - \{1-p_1(h_a)\}\right] + T_3(h_a) - T_4(h_a)$$
$$\{\text{ third order correction }\} \tag{54}$$

Continuing in this vein we get the following exact result,

$$P_{\downarrow\downarrow}(1\downarrow|0\downarrow;h_a) = e^{-p_0(h_a)} - \left[e^{-p_1(h_a)} - \{1-p_1(h_a)\}\right] - \sum_{n=3}^{\infty}(-1)^n T_n(h_a)$$
$$\{\text{ exact result }\} \qquad (55)$$

where

$$T_n(h_a) =$$
$$\int_{-2|J|-h_a}^{-h_a}\phi(h_1)dh_1\left[\prod_{m=3}^{n-1}\int_{h_{m-2}+2|J|}^{\infty}\phi(h_{m-1})dh_{m-1}\right]\int_{h_{n-2}+2|J|}^{\infty}\tilde{\phi}(h_{n-1})dh_{n-1} \qquad (56)$$

The probability per site of finding a doublet on the chain is equal to,

$$P_{\downarrow\downarrow}(h_a) = [P_{\downarrow\downarrow}(1\downarrow|0\downarrow:h_a)]^2 \qquad (57)$$

Note that although the (unconditional) probability of a doublet is the product of two mutually conditional probabilities, our notation for this is $P_{\downarrow\downarrow}(h_a)$ (without the square sign). In general it is not possible to do the integrals exactly to get an analytic expressions for $T_n(h_a)$ in a closed form. These have to be evaluated numerically. However T_n decreases exponentially with increasing n. In our numerical work we included terms up to $n \leq 4$ in the calculation of the conditional probability $P_{\downarrow\downarrow}(1\downarrow|0\downarrow:h_a)$, and used the square of

this quantity to calculate the probability per site of doublets. This gives an excellent fit with the simulation data as shown in section VI.

Although a doublet at an applied field h_a is the most basic object in our calculations but we need to calculate the probability of several other objects before we can calculate the magnetization curve. In order to calculate the magnetization curve we need to know the probability $P_\uparrow(h_a)$ that a randomly chosen site is up at h_a. On the lower half of the hysteresis loop, it is more convenient to focus on the complementary probability [1-$P_\uparrow(h_a)$] that a randomly chosen site is down. The randomly chosen site can have both its neighbors down, or both of them up, or one up and one down. If both neighbors of a down site are down, the site in question is necessarily a white site. The probability (per site) that a site is white is equal to $1 - p_0(h_a)$. Given a white site, the probability that both its neighbors are down is given by,

$$P_{\downarrow\downarrow\downarrow}(h_a) = [1 - p_0(h_a)]P\downarrow\downarrow(h_a) \tag{58}$$

Next, consider a down spin with one neighbor up and one down. In both cases there is a doublet, and the up spin is either to the left of the doublet or to its right. We have calculated the probability of a doublet as well as a triplet. From these we can obtain the probability of a doublet followed by an up spin using the equation

$$P_{\downarrow\downarrow\uparrow}(h_a) = P_{\downarrow\downarrow}(h_a) - P_{\downarrow\downarrow\downarrow}(h_a) \tag{59}$$

Naturally $P_{\downarrow\downarrow\uparrow}(h_a) = P_{\uparrow\downarrow\downarrow}(h_a)$ by symmetry.

Substituting from equations (58), we get

$$P_{\downarrow\downarrow\uparrow}(h_a) = P_{\uparrow\downarrow\downarrow}(h_a) = p_0(h_a)P_{\downarrow\downarrow}(h_a) \tag{60}$$

Note that the up spin in the above object could have flipped up under a p_0 or a p_1 process. We have checked the above equations against numerical simulations and the agreement is excellent as may be expected.

VI. Singlets

Now we calculate the probability $P_{\uparrow\downarrow\uparrow}(h_a)$ that a randomly chosen site is down and both its neighbors are up. Let the three consecutive sites that form this singlet be labeled $1, 2, 3$ and h_1, h_2, and h_3 denote the respective quenched fields. Without loss of generality we can assume that just before this singlet is created site-1 was up and sites 2 and 3 were down as shown in figure (14), i.e. site-1 flips up before site-3. We have to know if site-1 has flipped up under a p_0-process or a p_1-process. We consider both these possibilities for site-1 as well as site-3. The case when site-2 has never flipped in the course of applied field changing from $-\infty$ to h_a is somewhat simpler to analyze. Even in this case the probability $P_{\uparrow\downarrow\uparrow}(h_a)$ depends on whether (i) both neighbors flipped up under a p_0-process, or (ii)both neighbors flipped up under a p_1-process, or (iii) one neighbor flipped up under p_0-process and the other under a p_1-process. In the case (iii) it is also important whether the neighbor that flipped up first flipped under a p_0-process or a p_1-process. Indeed we require the following objects before we can calculate $P_{\uparrow\downarrow\uparrow}(h_a)$ in the simpler case mentioned above.

- $P_{\uparrow\downarrow\uparrow A}$ The fraction of singlets at applied field h_a when site-1 is up by a p_0 or a p_1-process and site-3 flips up by a p_0-process.
- $P_{\uparrow\downarrow\uparrow B}$ Fraction of $P_{\uparrow\downarrow\uparrow A}$ that are black at creation.

- $P_{\uparrow\downarrow\uparrow C}$ Fraction of $P_{\uparrow\downarrow\uparrow A}$ that are white at creation.

- $P_{\uparrow\downarrow\uparrow D}$ The fraction of singlets at applied field h_a when site-1 is up by a p_0 or a p_1-process and site-3 flips up next by a p_1-process.

- $P_{\uparrow\downarrow\uparrow E}$ Fraction of $P_{\uparrow\downarrow\uparrow D}$ that are black at creation.

- $P_{\uparrow\downarrow\uparrow F}$ Fraction of $P_{\uparrow\downarrow\uparrow D}$ that are white at creation ($P_{\uparrow\downarrow\uparrow D} - P_{\uparrow\downarrow\uparrow E}$).

- $P_{\uparrow\downarrow\uparrow G}$ The fraction of singlets at applied field h_a when site-1 and site-3 flip up by a p_0-process and site-2 is white.

- $P_{\uparrow\downarrow\uparrow H}$ The fraction of singlets at applied field h_a when site-1 flips up by a p_1-process, site-3 by a p_0-process, and site-2 is white. Site-1 flips up before site-3.

- $P_{\uparrow\downarrow\uparrow I}$ The fraction of singlets $P_{\uparrow\downarrow\uparrow C}$ that are white at their creation but are black at h_a.

- $P_{\uparrow\downarrow\uparrow J}$ The fraction of singlets at applied field h_a when site-1 and site-3 flip up by a p_1-process and site-2 is white.

- $P_{\uparrow\downarrow\uparrow K}$ The fraction of singlets at applied field h_a when site-1 flips up by a p_1-process, site-3 by a p_0-process, and site-2 is white. Site-3 flips up before site-1.

- $P_{\uparrow\downarrow\uparrow L}$ The fraction of singlets $P_{\uparrow\downarrow\uparrow F}$ that are white at their creation but are black at h_a.

- $P_{\uparrow\uparrow\uparrow M}$ Destruction of singlets associated with $P_{\uparrow\downarrow\uparrow B}$. By destruction we mean the disappearance of a singlet due to the down spin flipping up under a p_2-process.

- $P_{\uparrow\uparrow\uparrow N}$ Destruction of singlets associated with $P_{\uparrow\downarrow\uparrow E}$.

- $P_{\uparrow\uparrow\uparrow O}$ Destruction of singlets associated with $P_{\uparrow\downarrow\uparrow C}$.

- $P_{\uparrow\uparrow\uparrow P}$ Destruction of singlets associated with $P_{\uparrow\downarrow\uparrow F}$.

Up to this point we have focused on singlet sites that have never flipped starting from the saturated state at $h_a = -\infty$. In other words we have considered configurations comprising site-1 up, site-2 down, site-3 up where site-2 has never flipped up in increasing field from $-\infty$ to h_a. However, the anti-ferromagnetic dynamics also allows a singlet with site-2 having flipped twice i.e. site-2 can flip up and flip down again in the course of monotonically increasing applied field. In order to take into account the analysis of this second category of singlets, we need to calculate the following objects that are defined with respect to figures (15), (16), and (17).

- $P_{\uparrow\downarrow\uparrow Q}$ This object refers to figure (15) with the proviso that $h_2 > h_1$, $h_4 > h_5$, $h_4 > h_2$ ($h_4 < h_2$ will give an equal contribution). Site-3 flips first, site-4 flips next, site-2 flips after site-4 causing site-3 to flip down. $P_{\uparrow\downarrow\uparrow Q}$ refers to the fraction of singlets created in this way.

- $P_{\uparrow\downarrow\uparrow R}$ This object refers to figure (16) with the proviso that $h_2 > h_3$, $h_4 > h_3$, $h_4 > h_2$ ($h_4 < h_2$ will give an equal contribution). Site-3 flips first, site-4 flips next, site-2 flips after site-4 causing site-3 to flip down. $P_{\uparrow\downarrow\uparrow R}$ refers to the fraction of singlets created in this way.

- $P_{\uparrow\downarrow\uparrow S}$ This object refers to figure (17) with the proviso that $h_2 < h_3$, $h_4 > h_3$. Site-3 flips first, site-2 flips next, site-4 flips after site-2 causing site-3 to flip down. $P_{\uparrow\downarrow\uparrow S}$ refers to the fraction of singlets created in this way.

- $P_{\uparrow\downarrow\uparrow T}$ This object also refers to figure (17) with the proviso that $h_2 < h_3$, $h_4 > h_3$. Site-3 flips first, site-4 flips next, site-2 flips after site-4 causing site-3 to flip down. $P_{\uparrow\downarrow\uparrow T}$ refers to the fraction of singlets created in this way.

- $P_{\uparrow\uparrow\uparrow U}$ This object refers to the destruction of singlets associated with $P_{\uparrow\downarrow\uparrow Q}$.

- $P_{\uparrow\uparrow\uparrow V}$ This object refers to the destruction of singlets associated with $P_{\uparrow\downarrow\uparrow R}$.

- $P_{\uparrow\uparrow\uparrow W}$ This object refers to the destruction of singlets associated with $P_{\uparrow\downarrow\uparrow S}$.

- $P_{\uparrow\uparrow\uparrow X}$ This object refers to the destruction of singlets associated with $P_{\uparrow\downarrow\uparrow T}$.

A. $P_{\uparrow\downarrow\uparrow A}$

In an increasing applied field the objects associated with $P_{\uparrow\downarrow\uparrow A}$ are created from objects associated with $P_{\downarrow\downarrow\uparrow}$ and $P_{\uparrow\downarrow\downarrow}$ when the down site at one end of these objects flips up under a p_0-process. Suppose site-3 flips up under a p_0-process at h' $(-\infty \leq h' \leq h_a)$. Then we have $h_3 + 2|J| + h' = 0$ with probability $\phi(-2|J| - h')$. Thus,

$$\begin{aligned} P_{\uparrow\downarrow\uparrow A}(h_a) &= \int_{-\infty}^{h_a} [P_{\downarrow\downarrow\uparrow}(h') + P_{\uparrow\downarrow\downarrow}(h')]\phi(-h' - 2|J|)dh' \\ &= \int_{-\infty}^{h_a} 2p_0(h')P_{\downarrow\downarrow}(h')\phi(-h' - 2|J|)dh' \end{aligned} \tag{61}$$

where we have used equation (60). As a check we note that equation (60) is recovered by differentiating equation (61) with respect to h_a.

B. $P_{\uparrow\downarrow\uparrow B}$

This quantity is given by the equation.

$$\begin{aligned} P_{\uparrow\downarrow\uparrow B}(h_a) = 2\int_{-\infty}^{h_a} &[P_{\downarrow\downarrow}(2\downarrow|3\downarrow: h') - \{1 - p_0(h')\}] \\ &P_{\downarrow\downarrow}(4\downarrow|3\downarrow: h')\phi(-h' - 2|J|)dh' \end{aligned} \tag{62}$$

The explanation of the above equation is as follows. The in-

tegrand comprises three factors. The last factor is the prob that site-3 flips up at h' under a p_0-process. The other factors take into account that site-2 and site-4 (the right neighbor of site-3) are down at h' and site-2 is black: $\phi(-h'-2|J|)dh'$ is the probability that site-3 flips up at h'; $P_{\downarrow\downarrow}(2\downarrow|3\downarrow:h')-\{1-p_0(h')\}$ is the probability that site-2 is down and black ($h_2+2|J|+h'>0$); $P_{\downarrow\downarrow}(4\downarrow|3\downarrow;h')$ is the probability that site-4 is down.

C. $P_{\uparrow\downarrow\uparrow C}$

This is simply equal to $P_{\uparrow\downarrow\uparrow A}-P_{\uparrow\downarrow\uparrow B}$ but the notation is useful in the following analysis.

$$P_{\uparrow\downarrow\uparrow C}(h_a)=P_{\uparrow\downarrow\uparrow A}(h_a)-P_{\uparrow\downarrow\uparrow B}(h_a) \tag{63}$$

D $P_{\uparrow\downarrow\uparrow D}$

The singlets in this category are generated by doublets that are bordered by up spins at both ends. Thus site-1 is up, site-2 and site-3 are down, and site-4 is up. Site-2 and site-3 are on equal footing and therefore the *a posteriori* distribution of quenched fields $\tilde{\phi}(h_2)$ and $\tilde{\phi}(h_3)$ are identical. We can assume without loss of generality that $h_3>h_2$ and multiply the result by a factor 2. Thus we focus on a singlet created at site-2 when site-3 flips up at h' ($-\infty<h'\leq h_a$). We get,

$$P_{\uparrow\downarrow\uparrow D}(h_a) = 2\int_{-\infty}^{h_a} dh' \tilde{\phi}(-h') p_0(h') P_{\downarrow\downarrow}(2\downarrow|3\downarrow; h') \qquad (64)$$

The explanation of the above equation is as follows: $\tilde{\phi}(-h')$ is the probability that site-3 flips up at $h' + h_3 = 0$; $p_0(h')P_{\downarrow\downarrow}(2\downarrow|3\downarrow; h')$ is the probability that site-2 is down and site-1 is up just before site-3 flips up. The *a posteriori* distribution $\tilde{\phi}(h')$ may be obtained by differentiating the following equation.

$$\int_{-h'}^{\infty} dh_3 \tilde{\phi}(h_3) = \left[e^{-p_1(h')} - \{1 - p_1(h')\}\right] - \sum_{n=3}^{\infty} (-1)^n \tilde{T}_n(h' - 2|J|) \qquad (65)$$

where,

$$\tilde{T}_n(h') = \int_{-2|J|-h'}^{\infty} \phi(h_1) dh_1 \times \left[\prod_{m=3}^{n-1} \int_{h_{m-2}+2|J|}^{\infty} \phi(h_{m-1}) dh_{m-1}\right] \int_{h_{n-2}+2|J|}^{\infty} \tilde{\phi}(h_{n-1}) dh_{n-1} \qquad (66)$$

We may rewrite equation (55) as

$$P_{\downarrow\downarrow}(1\downarrow|0\downarrow; h') = e^{-p_0(h')} - \left[e^{-p_1(h')} - \{1 - p_1(h')\}\right] - \sum_{n=3}^{\infty} (-1)^n \left[\tilde{T}_n(h') - \tilde{T}_n(h' - 2|J|)\right] \qquad (67)$$

For spins flipping up under a p_1-process only the second and the last term on the right hand side comes into play.

E. $P_{\uparrow\downarrow\uparrow E}$

Here we want the fraction of singlets in section D that are created black. If h' is the field at which site-3 flips by p_1-process then the cumulative fraction of singlets which are black at creation is given by

$$P_{\uparrow\downarrow\uparrow E}(h_a) = 2\int_{-\infty}^{h_a} dh' \tilde{\phi}(-h') \left[P_{\downarrow\downarrow}(2\downarrow|3\downarrow;h') - \{1 - p_0(h')\}\right] \quad (68)$$

The first factor in the integrand gives the probability that $h_3 + h' = 0$, and the second factor gives the probability that site-2 is down and black at h'.

F. $P_{\uparrow\downarrow\uparrow F}$

$$P_{\uparrow\downarrow\uparrow F}(h_a) = P_{\uparrow\downarrow\uparrow D}(h_a) - P_{\uparrow\downarrow\uparrow E}(h_a) \quad (69)$$

G. $P_{\uparrow\downarrow\uparrow G}$

If a site is white with probability $1 - p_0(h_a)$ then it is down with probability unity. The probability that either of its neighbor is down under a p_0-process alone is equal to $e^{-p_0(h_a)}$. Thus the probability

that either of its neighbor is up under a p_0-process alone is equal to $1 - e^{-p_0(ha)}$. Therefore,

$$P_{\uparrow\downarrow\uparrow G}(h_a) = \{1 - p_0(h_a)\}[1 - e^{-p_0(h_a)}]^2 \tag{70}$$

H. $P_{\uparrow\downarrow\uparrow H}$

$$P_{\uparrow\downarrow\uparrow H}(h_a) = 2\{1 - p_0(h_a)\} \int_{-\infty}^{h_a} dh' P_{\downarrow\downarrow}(3\downarrow|2\downarrow; h')\phi(-2|J| - h') \times \int_{-\infty}^{h'} \tilde{\phi}(-h'')dh'' \tag{71}$$

The above equation is understood as follows. The integral over h'' takes care of the site flipping up under a p_1-process at h''. Therefore the density associated with this integral is the *a posteriori* distribution $\tilde{\phi}(-h'')$. Site flipping up under the p_0-process flips up at h' where $h' > h''$.The density associated with this site is $P_{\downarrow\downarrow}(3\downarrow|2\downarrow; h')\phi(-2|J| - h')$. The first factor accounts for the fact that the site in question is down given that it is next to a down site (the white site with probability $1 - p_0(h_a)$ and the second factor accounts for the fact that although it is down it is on the verge of turning up at h' under a p_0-process. Finally the factor 2 takes care of an equivalent configuration in which the location of sites flipping up under a p_0 and a p_1-process are interchanged.

I. $P_{\uparrow\downarrow\uparrow I}$

The fraction of singlets $P_{\uparrow\downarrow\uparrow C}$ that are white at their creation but black at h_a is given by,

$$P_{\uparrow\downarrow\uparrow I} = P_{\uparrow\downarrow\uparrow C} - P_{\uparrow\downarrow\uparrow G} - P_{\uparrow\downarrow\uparrow H} \tag{72}$$

J. $P_{\uparrow\downarrow\uparrow J}$

$$P_{\uparrow\downarrow\uparrow J}(h_a) = [1 - p_0(h_a)] \left[\int_{-h_a}^{\infty} dh_3 \tilde{\phi}(h_3) \right]^2 \tag{73}$$

The first factor takes into account that the singlet site is white. The second factor gives the probability that both neighbors of the down site flip up under a p_1-process.

K. $P_{\uparrow\downarrow\uparrow K}$

$P_{\uparrow\downarrow\uparrow K}$ may be obtained on similar lines as $P_{\uparrow\downarrow\uparrow H}$. We get,

$$\begin{aligned} P_{\uparrow\downarrow\uparrow K}(h_a) &= 2\{1 - p_0(h_a)\} \int_{-\infty}^{h_a} dh' \tilde{\phi}(-h') \\ &\times \int_{-\infty}^{h'} dh'' P_{\downarrow\downarrow}(3 \downarrow | 2 \downarrow; h'') \phi(-h'' - 2|J|) \end{aligned} \tag{74}$$

L. $P_{\uparrow\downarrow\uparrow L}$

The fraction of singlets $P_{\uparrow\downarrow\uparrow F}$ that are white at their creation but black at h_a is given by,

$$P_{\uparrow\downarrow\uparrow L} = P_{\uparrow\downarrow\uparrow F} - P_{\uparrow\downarrow\uparrow J} - P_{\uparrow\downarrow\uparrow K} \tag{75}$$

M. $P_{\uparrow\uparrow\uparrow M}$

We now turn to the destruction i.e. the disappearance of a singlet due to the down spin flipping up under a p_2-process. We start with the destruction of singlets associated with $P_{\uparrow\downarrow\uparrow B}$. Taking into account the inequalities $h_2 - 2|J| < h_3 < h_2$ that require site-2 to be down and a black site when site-3 flips up, we get

$$P_{\uparrow\uparrow\uparrow M}(h_a) = 2\int_{-\infty}^{h_a} dh'\tilde{\phi}(-h'+2|J|)$$
$$\times \int_{h'-4|J|}^{h'-2|J|} dh''\phi(-h''-2|J|)P_{\downarrow\downarrow}(3\downarrow|2\downarrow;h'') \tag{76}$$

N. $P_{\uparrow\uparrow\uparrow N}$

We now turn to the destruction of singlets associated with $P_{\uparrow\downarrow\uparrow E}$. These singlets were created under the condition $h_2+2|J| > h_3 > h_2$. They will be destroyed at $h_2 - 2|J| + h' = 0$ with the probability $\tilde{\phi}(-h'+2|J|)$. Thus the cumulative fraction of the destroyed singlets at h_a is given by,

$$P_{\uparrow\uparrow\uparrow N}(h_a) = 2\int_{-\infty}^{h_a} dh'\tilde{\phi}(-h'+2|J|)\int_{h'-4|J|}^{h'-2|J|} dh''\tilde{\phi}(-h'') \qquad (77)$$

O. $P_{\uparrow\uparrow\uparrow O}$

We now consider the destruction of singlets associated with $P_{\uparrow\downarrow\uparrow C}$. Recall that $P_{\uparrow\downarrow\uparrow C}$ are white at creation. A fraction $P_{\uparrow\downarrow\uparrow I}$ of these become black, say at h' i.e. these can flip up at h' under a p_0-process if they were to have both neighbors down. However they have both neighbors up. Therefore they would flip up at applied field $h_a = h' + 4|J|$. Thus we get,

$$P_{\uparrow\uparrow\uparrow O} = P_{\uparrow\downarrow\uparrow I}(h_a - 4|J|) \qquad (78)$$

P. $P_{\uparrow\uparrow\uparrow P}$

$P_{\uparrow\uparrow\uparrow P}$ represents the destruction of singlets associated with $P_{\uparrow\downarrow\uparrow F}$. This is similar to the preceding case because $P_{\uparrow\downarrow\uparrow F}$ are also white at creation. Following similar reasoning as used in the preceding section,

$$P_{\uparrow\uparrow\uparrow P} = P_{\uparrow\downarrow\uparrow L}(h_a - 4|J|) \qquad (79)$$

Q. $P_{\uparrow\downarrow\uparrow Q}$

Refer to figure (15) and the definition of $P_{\uparrow\downarrow\uparrow Q}$. We have $h_1 < h_2$, $h_5 < h_4$. The screening property of doublets ensures that the evolution of sites 2, 3, and 4 is uninfluenced by sites 1 and 5. Also, $h_3 > h_4 > h_2$ for site-3 to have flipped up before sites 2 and 4 ($h_3 > h_2 > h_4$ would make an equal contribution). Now site-2 flips up at h_a and site-3 flips down. Therefore, $h_2 + h_a = 0$, and $h_3 - 2|J| + ha < 0$. Consequently $h_3 - h_2 < 2|J|$, $h_4 < h_3 < h_2 + 2|J|$, and $h_2 < h_4 < h_2 + 2|J|$. The probability that site-3 would flip down when site-2 flips up is given by

$$P_{\uparrow\downarrow\uparrow Q}(h_a) = 2\int_{-\infty}^{h_a} dh'\phi(-h')P_{\downarrow\downarrow}(1\downarrow|2\downarrow;h')$$
$$\times \int_{h'-2|J|}^{h'} dh''\phi(-h'')P_{\downarrow\downarrow}(5\downarrow|4\downarrow;h'')\int_{-h''}^{-h'+2|J|} dh'''\phi(-h'''-2|J|) \quad (80)$$

The limits on the integrals were discussed just before the equation. Note that one can use the quenched field at a site as a variable of integration or equivalently the applied field at which the site in question flips up. We have written the integrals in terms of the applied fields h''', h'', h' at which sites 3 , 4, and 2 flip up respectively ($h''' < h'' < h'$). The explanation of the integrands is as follows. The integrand in the last integral is the probability that site-3 flipped up by a p_0-process at $h_3 + 2|J| + h''' = 0$. The second integrand is

the probability that site-4 flips up at $h_4 + h'' = 0$ and site-5 is down. Similarly the first integrand is the probability that site-2 flips up at h' and site-1 is down.

R. $P_{\uparrow\downarrow\uparrow R}$

Refer to figure (16) and the definition of $P_{\uparrow\downarrow\uparrow R}$. Our object is to calculate the probability that site-3 flips down when site-2 and site-4 are up. This happens only if site-3 flips up after site-1 and site-5, i.e. sites 2, 3, 4 form a string of three down spins bordered by up spins at 1 and 5 just before 3 flips up. Because sites 2 and 4 are adjacent to up spins the distribution of h_2 and h_4 is the *a posteriori* $\tilde{\phi}(h_2)$ and $\tilde{\phi}(h_4)$ respectively. Also $h_3 > h_2 - 2|J|$ and $h_3 > h_4 - 2|J|$ because 3 flips up before 2 and 4. We assume $h_4 > h_2$ and multiply our result by a factor of 2 to include the case $h_4 < h_2$. Thus $h_4 - 2|J| < h_3 < h_2$, $h_4 - h_2 < 2|J|$, and $h_2 < h_4 < h_2 + 2|J|$. The probability that site-3 flips down when site-2 flips up is given by

$$P_{\uparrow\downarrow\uparrow R}(h_a) = 2\int_{-\infty}^{h_a} dh'\tilde{\phi}(-h' + 2|J|)\int_{h'-2|J|}^{h'} dh''\tilde{\phi}(-h'' + 2|J|) \times \int_{-h''}^{-h'+2|J|} dh'''\phi(-h''' - 2|J|) \qquad (81)$$

The integrand of the first and the second integral is the probability that site-2 and site-4 flip up by a p_2-process at h' and h''

respectively. The last integrand is the probability that site-3 flips up by a p_0- process at h'''.

S. $P_{\uparrow\downarrow\uparrow S}$

In figure(17) site-2 or site-4 could flip up first. Let us consider the case when site-2 flips up first i.e. $h_2 > h_4 - 2|J|$. $P_{\uparrow\downarrow\uparrow S}$ is zero unless $h_2 < h_3 < h_4$ and $h_4 - 2|J| < h_2 < h_4$. Therefore the probability that a new singlet is created at site-3 when site-4 flips up is given by

$$P_{\uparrow\downarrow\uparrow S}(h_a) = 2\int_{-\infty}^{h_a} dh'\tilde{\phi}(-h'+2|J|)\int_{h'-2|J|}^{h'} dh''\phi(-h'')P_{\downarrow\downarrow}(1\downarrow|2\downarrow;h'') \times \int_{-h''}^{-h'+2|J|} dh'''\phi(-h'''-2|J|) \qquad (82)$$

The last integrand has the same interpretation as in the previous object $P_{\uparrow\downarrow\uparrow R}$. The second integrand is the probability that site-1 is down when site-2 flips up by a p_1-process at h''. Finally the first integrand is the probability that site-4 flips up by a p_2-process at h'

T. $P_{\uparrow\downarrow\uparrow T}$

Site-4 would flip up before site-2 in figure(17) if $h_4 > h_2 + 2|J|$. Clearly $h_3 > h_2$. Site-3 would flip down when site-2 flips up if $h_3 < h_2 + 2|J|$. Thus h_3 and h_4 lie in the range $h_4 - 2|J| < h_3 < h_2 + 2|J|$

and $h_2 + 2|J| < h_4 < h_2 + 4|J|$. The probability that site-3 flips down when site-2 flips up is given by

$$P_{\uparrow\downarrow\uparrow T}(h_a) = 2\int_{-\infty}^{h_a} dh'\phi(-h')P_{\downarrow\downarrow}(1\downarrow|2\downarrow;h')\int_{h'-2|J|}^{h'} dh''\tilde{\phi}(-h''+2|J|) \times \int_{-h''}^{-h'+2|J|} dh'''\phi(-h'''-2|J|) \qquad (83)$$

The integrand is similar to that in $P_{\uparrow\downarrow\uparrow S}$ except that the first integral is for h_2 and the second for h_4.

U. $P_{\uparrow\uparrow\uparrow U}$

$P_{\uparrow\uparrow\uparrow U}$ is associated with the destruction of objects characterized by $P_{\uparrow\downarrow\uparrow Q}$. The destruction can be analyzed on similar lines as their creation except that we now have the inequalities $h_2 < h_4 < h_3$ and $h_3 - 2|J| < h_2 < h_3$. The probability that site-3 in $P_{\uparrow\downarrow\uparrow Q}$ flips for the third time is given by

$$P_{\uparrow\uparrow\uparrow U}(h_a) = 2\int_{-\infty}^{h_a} dh'\phi(-h'+2|J|)\int_{h'-2|J|}^{h'} dh''\phi(-h'')P_{\downarrow\downarrow}(1\downarrow|2\downarrow;h'') \times \int_{h'-2|J|}^{h''} dh'''\phi(-h''')P_{\downarrow\downarrow}(5\downarrow|4\downarrow;h''') \qquad (84)$$

The second and the third integrands give the probability that sites 2 and 4 flip up at h'' and h''' respectively. The first integrand is the probability that site-3 flips up by a p_2-process at h'. Note that

a priori distributions $\phi(h_2), \phi(h_3), \phi(h_4)$ are used here because these sites have remained screened from site-1 and site-5.

V. $P_{\uparrow\uparrow\uparrow V}$

$P_{\uparrow\uparrow\uparrow V}$ is associated with the destruction of $P_{\uparrow\downarrow\uparrow R}$. The inequalities that govern $P_{\uparrow\uparrow\uparrow V}$ are $h_2 < h_4 < h_3 + 2|J|$ and $h_3 < h_2 < h_3 + 2|J|$. Thus the probability that the down spin in $P_{\uparrow\downarrow\uparrow R}$ flips for the third time is

$$P_{\uparrow\uparrow\uparrow V}(h_a) = 2\int_{-\infty}^{h_a} dh'\phi(-h' + 2|J|)\int_{h'-2|J|}^{h'} dh''\tilde{\phi}(-h'' + 2|J|) \times \int_{h'-2|J|}^{h''} dh'''\tilde{\phi}(-h''' + 2|J|) \qquad (85)$$

The second and the third integrands give the probability that site-2 and site-4 flip up by a p_2-process at h'' and h''' respectively. The first integrand is the probability that site-3 flips up by a p_2-process at h'.

W. $P_{\uparrow\uparrow\uparrow W}$

$P_{\uparrow\uparrow\uparrow W}$ is associated with the destruction of $P_{\uparrow\downarrow\uparrow S}$. The appropriate inequalities for $P_{\uparrow\uparrow\uparrow W}$ are $h_3 < h_4 < h_3 + 2|J|$ and $h_4 - 2|J| < h_2 < h_3$. The probability that the down spin in question flips for the third time is

$$P_{\uparrow\uparrow\uparrow W}(h_a) = 2\int_{-\infty}^{h_a} dh'\phi(-h'+2|J|)\int_{h'-2|J|}^{h'} dh''\tilde{\phi}(-h''+2|J|)$$
$$\times\int_{h'-2|J|}^{h''} dh'''\phi(-h''')P_{\downarrow\downarrow}(1\downarrow|2\downarrow;h''') \qquad (86)$$

The first integrand is the probability that site-3 flips up by a p_2-process at h'. The second and third integrands account for site-4 and site-2 respectively.

X. $P_{\uparrow\uparrow\uparrow X}$

$P_{\uparrow\uparrow\uparrow X}$ gives the fraction of singlets associated with $P_{\uparrow\downarrow\uparrow T}$ that are destroyed at h_a. These may be calculated in a similar manner as in the preceding case. We now have the inequalities $h_2 + 2|J| < h_4 < h_3 + 2|J|$ and $h_3 - 2|J| < h_2 < h_3$. Therefore the probability that the down spin in $P_{\uparrow\downarrow\uparrow T}$ flips up is given by,

$$P_{\uparrow\uparrow\uparrow X}(h_a) = 2\int_{-\infty}^{h_a} dh'\phi(-h'+2|J|)\int_{h'-2|J|}^{h'} dh''\phi(-h'')P_{\downarrow\downarrow}(1\downarrow|2\downarrow;h'')$$
$$\times\int_{h'-2|J|}^{h''} dh'''\tilde{\phi}(-h'''+2|J|) \qquad (87)$$

The last two integrands pertain to sites 2 and 4 respectively, and the first to site-3.

VII. Magnetization on lower hysteresis loop

We are now in a position to write the magnetization on the lower half of the hysteresis loop.

$$m(h_a) = 1 - 2P_{\downarrow}(h_a) \tag{88}$$

where $P_{\downarrow}$ is the probability that a randomly chosen site on the chain is down at applied field h_a. A randomly chosen site on the chain can be characterized by the number n of up neighbors it has $(n = 0, 1, 2)$. Thus we can write,

$$P_{\downarrow}(h_a) = P_{\downarrow\downarrow\downarrow}(h_a) + P_{\downarrow\downarrow\uparrow}(h_a) + P_{\uparrow\downarrow\downarrow}(h_a) + P_{\uparrow\downarrow\uparrow}(h_a) \tag{89}$$

The first term corresponds to $n = 0$, the next two terms that are equal by symmetry correspond to $n = 1$, and the last term corresponds to $n = 2$. We obtained the first three terms on the right-hand-side with relative ease in section (V). Surprisingly the evaluation of the last term i.e. $P_{\uparrow\downarrow\uparrow}(h_a)$ proved rather tedious requiring the calculation of 24 terms as a pre-requisite $[P_{\uparrow\downarrow\uparrow A}(h_a)$ to $P_{\uparrow\uparrow\uparrow X}(h_a)]$. We have (so far) not found a simpler method to calculate $P_{\uparrow\downarrow\uparrow}(h_a)$ in spite of much effort and thought. Putting all terms together we get,

$$
\begin{aligned}
P_{\downarrow}(h_a) = P_{\downarrow\downarrow\downarrow}(h_a) + P_{\downarrow\downarrow\uparrow}(h_a) + P_{\uparrow\downarrow\downarrow}(h_a) + P_{\uparrow\downarrow\uparrow A}(h_a) + P_{\uparrow\downarrow\uparrow D}(h_a) \\
-P_{\uparrow\uparrow\uparrow M}(h_a) - P_{\uparrow\uparrow\uparrow N}(h_a) - P_{\uparrow\uparrow\uparrow 0}(h_a) - P_{\uparrow\uparrow\uparrow P}(h_a) \\
+P_{\uparrow\downarrow\uparrow Q}(h_a) + P_{\uparrow\downarrow\uparrow R}(h_a) + P_{\uparrow\downarrow\uparrow S}(h_a) + P_{\uparrow\downarrow\uparrow T}(h_a) \\
-P_{\uparrow\uparrow\uparrow U}(h_a) - P_{\uparrow\uparrow\uparrow V}(h_a) - P_{\uparrow\uparrow\uparrow W}(h_a) - P_{\uparrow\uparrow\uparrow X}(h_a)
\end{aligned}
\tag{90}
$$

We note that several objects that we calculated in the preceding section do not appear explicitly in the above equation e.g. $P_{\uparrow\downarrow\uparrow B}(h_a)$ does not appear explicitly in equation (90). However it is necessary to calculate $P_{\uparrow\downarrow\uparrow B}(h_a)$ because it is needed in the calculation of $P_{\uparrow\downarrow\uparrow M}(h_a)$ and $P_{\uparrow\downarrow\uparrow O}(h_a)$ that appear in the final formula. Similar remarks apply to other terms that were calculated but do not appear explicitly in equation (90).

The magnetization in increasing field is obtained by substituting equation (90) into equation (88). The magnetization in decreasing field on the upper half of the hysteresis loop is given by symmetry,

$$
m^u(h_a) = -m(-h_a) \tag{91}
$$

In the next section we compare the theoretical result against numerical simulations of the model in selected cases. We consider a uniform bounded distribution of the quenched field as well as a

Gaussian distribution. As may be anticipated, the agreement between theory and numerical simulation is quite good.

VIII. Comparison with simulations and concluding remarks

Simulations of the model have played an important role in the analysis presented here. Although an exact analytic result has to be necessarily in agreement with the simulations within numerical errors but arguments based on conditional probabilities can be subtle and prone to errors. Therefore at each step of the analysis, we devised a simulation of the model to yield the probability of the event being calculated. Occasionally the two would not match in the first instance necessitating a rethink of the analysis and locating the error in the argument. Each of the theoretical expression in the preceding section was thus verified by simulation of the model for the following distributions of the random field: (i) bounded distribution with half-width $\Delta = 1.25|J|$ (ii) a Gaussian distribution with standard deviation $\sigma = .5|J|$. The average value of the random field is zero in both cases. The comparison between the theoretical hysteresis loops and the hysteresis loops obtained by simulation was shown already in section III. Here we show the comparison for a few intermediate quantities that were used to obtain the hysteresis loops.

We begin with the probability per site of a doublet on the lower half of the hysteresis loop. Figure (18) shows the theoretical expression for $P_{\downarrow\downarrow}(h_a)$ for the Gaussian distribution with the corresponding

data from numerical simulation superimposed on it. The fit is so close that the two are indistinguishable on the scale of the figure. Figures (19) and (20) show similar comparisons for uniform distributions for $\Delta = 1.25$ and $\Delta = 0.5$ respectively. In each of the following figures data from the corresponding numerical simulation has been plotted along side the theoretical expression. In most cases the match between theory and simulation is so good that there appears to be only a single curve in the figure. In other cases (when the probability of the event is relatively small and finite size corrections are larger) we can barely make out that there are two curves that almost lie on each other. Figures (21), (22), and (23) show the result for $P_{\downarrow\downarrow\downarrow}(h_a)$ for the Gaussian and uniform distributions with $\Delta = 1.25$ and $\Delta = 0.5$ respectively . Results for $P_{\uparrow\downarrow\downarrow}(h_a) + P_{\downarrow\downarrow\uparrow}(h_a)$ are shown in figures (24), (25) and (26). Figures (27), (28), and (29) show the comparison between theory and simulation for $P_{\uparrow\downarrow\uparrow A}(h_a)$ for a Gaussian as well as a uniform distribution. Figures (30), (31), and (32) shows similar comparison for $P_{\uparrow\downarrow\uparrow D}(h_a)$. Figure (33), (34), and (35) are for $P_{\uparrow\uparrow\uparrow M}(h_a)$. Figures (36), (37), and (38) are for $P_{\uparrow\uparrow\uparrow N}(h_a)$. Figures (39), (40), and (41) show $P_{\uparrow\downarrow\uparrow Q}(h_a)$. Figures (42), (43), and (44) show $P_{\uparrow\uparrow\uparrow U}(h_a)$. Finally, Figures (45), (46) and (47) show $P_{\uparrow\downarrow\uparrow W}(h_a)$. These figures and a few more that we have omitted here have played a very important role in the process of finding the exact magnetization.

In conclusion we have obtained the zero-temperature hysteresis

loop of a one dimensional anti-ferromagnetic random field Ising model in the case when the driving field varies from $-\infty$ to ∞ and back to $-\infty$ infinitely slowly. The problem is simple to state but difficult to solve. The end result for the hysteresis loop involves integrals that in general have to be evaluated numerically. We have shown that our theoretical results fit numerical simulations of the model quite well. However, several aspects of the problem still remain unsolved [43]. For example we have obtained the hysteresis loop when the driving field takes the system from one saturated state ($h_a = -\infty$) to another ($h_a = \infty$). In this case we have a complete knowledge of the *a posteriori* distribution of the quenched field at different stages of evolution of the system. We are not in a position (so far) to obtain the hysteretic response of the system starting from an arbitrary initial state. It would be interesting to have an analytic solution of the problem in higher dimensions as well. Numerical simulations suggest that the anti-ferromagnetic hysteresis loops in higher dimensions have several plateaus for low values of Δ and σ as compared with $|J|$. Exact analytic solutions of problems with quenched disorder are difficult in statistical mechanics. One may even argue if they are worth the effort that has to be put in to try to obtain them. However exact solutions are intellectually satisfying and provide a framework for understanding a wide class of complex phenomena. We hope there will be more progress in this direction in the future.

Bibliography

[1] *Statistical Mechanics: A set of lectures* by R P Feynman, W A Benjamin, Inc., Reading, Massachusetts, USA (1972).

[2] *Spinglasses and Random Fields*, ed. A P Young, World Scientific, Singapore (1997).

[3] Y Imry and S Ma Phys Rev Lett 35, 1399 (1975); for a more recent review of random field phenomena see e.g. T Nattermann in [2].

[4] D Sherrington and S Kirkpatrick, Phys Rev Lett 35, 1972 (1975).

[5] J P Sethna, K A Dahmen, S Kartha, J A Krumhansl, B W Roberts, and J D Shore, Phys Rev Lett 70, 3347 (1993); K Dahmen and J P Sethna, Phys Rev Lett 71, 3222(1993); O Perkovic, K Dahmen, and J P Sethna, Phys Rev Lett 75, 4528 (1995).

[6] J P Sethna, K A Dahmen, and O. Percovic in [13] and references therein.

[7] K A Dahmen and J P Sethna, Phys Rev B 53, 14872 (1996).

[8] P Shukla, Prog Theo Phys 96, 69-80 (1996).

[9] P Shukla, Physica A233, 235-241 (1996).

[10] D Dhar, P Shukla, and J P Sethna, J Phys A30, 5259 (1997).

[11] Prabodh Shukla and R S Kharwanlang, Phys Rev E 81, 031106 (2010).

[12] Prabodh Shukla and R S Kharwanlang, Phys Rev E 83, 011121 (2011).

[13] See for example, *The Science of Hysteresis*, edited by G Bertotti and I Mayergoyz, Academic Press, Amsterdam (2006).

[14] R J Glauber, J Math Phys 4, 294 (1963).

[15] K G Wilson, Phys Rev B4, 3174(1971); K G Wison, Phys Rev B4, 3184 (1971).

[16] See for example, E C Stoner, Rev Mod Phys 25, 2 (1953). The main features of Barkhausen noise discovered in these early experiments are still topics of current research.

[17] S Sabhapandit, D Dhar, and P Shukla, Phys Rev Lett 88, 197202 (2002).

[18] R da Silveira and M Kardar, Phys Rev E 59, 1355 (1999).

[19] R A da Silveira and S Zapperi, Phys Rev B 69, 212404 (2004).

[20] Zero-temperature hysteresis in an anti-ferromagnetic Ising chain with quenched random fields, P Shukla, Physica A233, 242-252 (1996).

[21] Hysteretic response of an anti-ferromagnetic random field Ising model in one dimension at zero temperature, Prabodh Shukla, Ratnadeep Roy, and Emilia Ray, Physica A 275, 380 (2000); cond-mat/9910021.

[22] item Hysteresis in one-dimensional anti-ferromagnetic random field Ising model at zero temperature, Prabodh Shukla, Ratnadeep Roy, and Emilia Ray, Physica A 276, 365 (2000); cond-mat/9910169.

[23] Driven Random Field Ising Model: some exactly solved examples in threshold activated kinetics, Prabodh Shukla, Int J Mod Phys B 17, 5583 (2003); cond-mat/0401252.

[24] Exact solution of return hysteresis loops in a one dimensional random-field Ising model at zero temperature, Prabodh shukla, Phys Rev E 62, 4725 (2000); cond-mat/0004125.

[25] Exact expressions for minor hysteresis loops in the random-field Ising model on a Bethe lattice at zero temperature, Prabodh Shukla, Phys Rev E 63, 27102 (2001); cond-mat/0007370.

[26] S Sabhapandit, P Shukla, and D Dhar, J Stat Phys 98, 103 (2000).

[27] X Illa, P Shukla, and E Vives, Phys Rev B 73, 092414 (2006).

[28] X Illa, M L Rosinberg, P Shukla, and E Vives, Phys Rev B 74, 224404 (2006).

[29] X Illa, M L Rosinberg, and G Tarjus, Eur Phys J B54, 355 (2006).

[30] P Ayyub et al, Phys Rev B 57, R5559 (1998).

[31] K Fukuma and M Torii, Earth Planets Space 50, 9 (1998).

[32] I Chiorescu et al, Phys Rev Lett 84, 3454 (2000).

[33] E E Fullerton et al, Appld Phys Lett 77, 3806(2000).

[34] O Waldmann et al, Phys Rev Lett 89, 246401(2002).

[35] K Takanashi, Appld Phys Lett 63, 1585 (1993).

[36] Khian-Hooi Chew et al, Appld Phys Lett 77, 2755 (2000).

[37] J Kisker,H Rieger, and H Schreckenberg, J Phys A: Math. Gen. 27, L853 (1994). This paper discusses the non-equilibrium dynamics of a non-random, one-dimensional Ising model, with three-spin interactions, at low temperatures. It is qualitatively similar to the dynamics of the random field Ising model at zero-temperature.

[38] H Reiger, Physica A 224, 267 (1996).

[39] F Ritort and P Sollich, Advances in Physics 52:4, 219 (2003).

[40] C Toninelli, PhD thesis (2003).

[41] J W Evans, Rev Mod Phys 65, 1281 (1993).

[42] L G Mityushin, Prob Peredachi Inf 9, 81 (1973). Also see reference (39) for a detailed discussion of the screening property of this class of problems.

[43] J M Deutsch, A Dhar, and O Narayan, Phys Rev Lett 92, 227203 (2004).

Figures

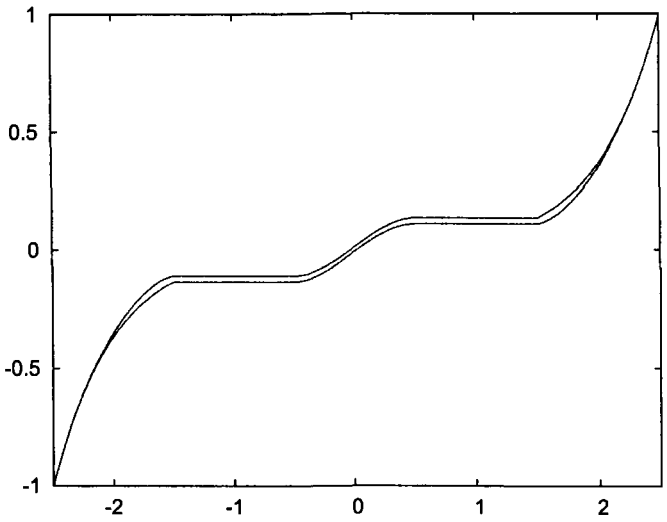

FIG. 1: Hysteresis loop for an anti-ferromagnetic random-field Ising model with $J = -1$ and $\Delta = 0.5$ (see text). The x-axis shows the applied field and the y-axis magnetization per spin. As $|J| \leq \Delta$, each half of the hysteresis loop comprises three ramps separated by two plateaus. The lower half of the loop shows magnetization in increasing field and the upper half in decreasing field. A theoretical expression has been superimposed on the numerical data.

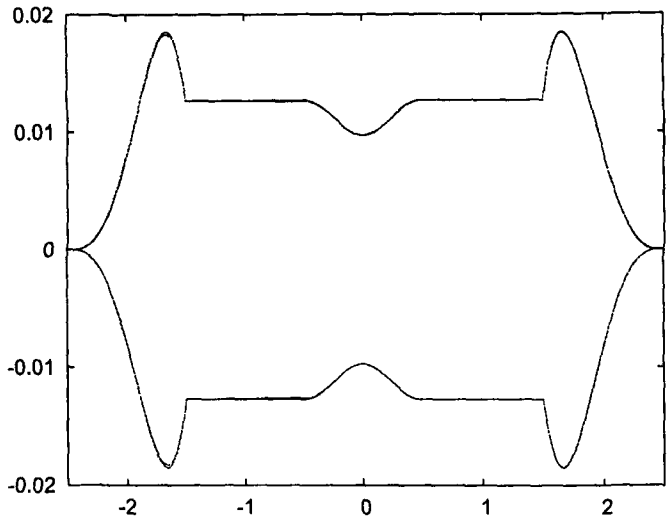

FIG. 2: A magnified view of the theoretical and simulation hysteresis loops for $\Delta = 0.5$ where the y-axis shows the magnetization in increasing and decreasing field as measured from the average of the magnetization on the lower and the upper half of the hysteresis loop in figure 1 at corresponding applied field.

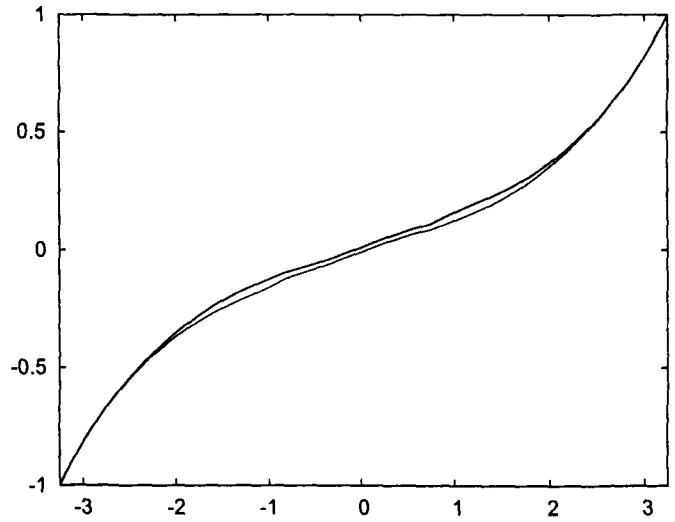

FIG. 3: Hysteresis loop for an anti-ferromagnetic random-field Ising model with $J = -1$ and $\Delta = 1.25$ (see text). The x-axis shows the applied field and the y-axis magnetization per spin. As $|J| > \Delta$, the plateaus of figure 1 disappear and the three ramps merge into each other. A theoretical expression has been superimposed on the numerical data.

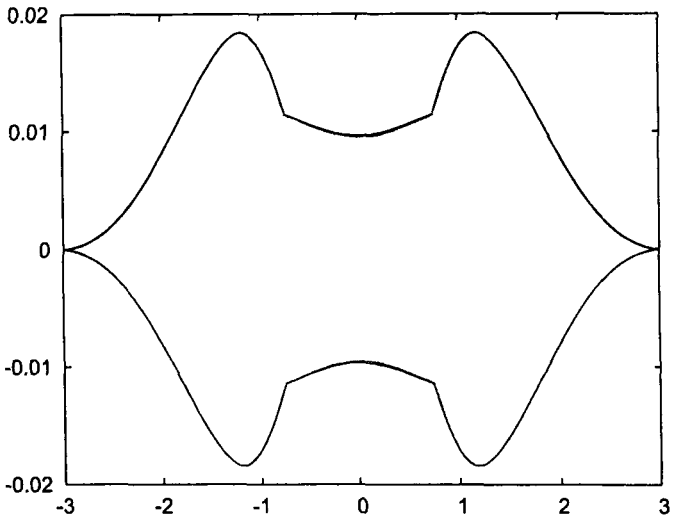

FIG. 4: Theoretical and simulation hysteresis loops for $\Delta = 1.25$ where the magnetization along increasing and decreasing field is measured from the average of the magnetization on the lower and the upper half of the hysteresis loop in figure 3 at corresponding applied field.

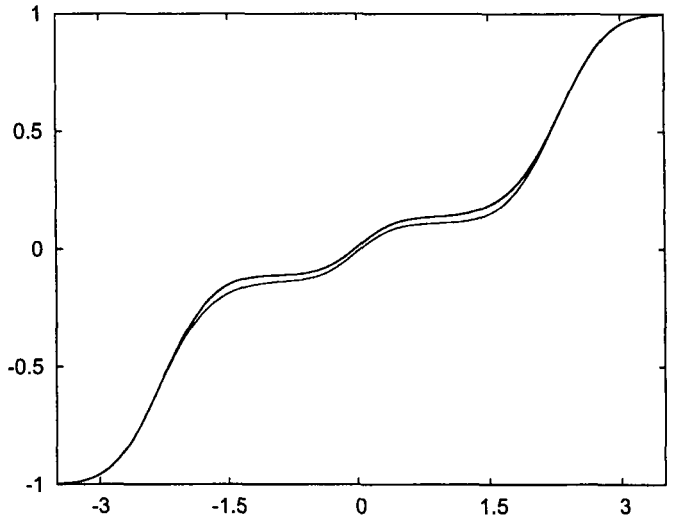

FIG. 5: Hysteresis loop for an anti-ferromagnetic random-field Ising model with $J = -1$ and $\sigma = 0.5$ (see text). Notice the approximate similarity with the hysteresis loop in figure 1 but the absence of sharp ramps and plateaus. For a Gaussian distribution the three ramps merge into each other for any value of σ although this is less pronounced at smaller values of σ. A theoretical expression has been superimposed on the numerical data.

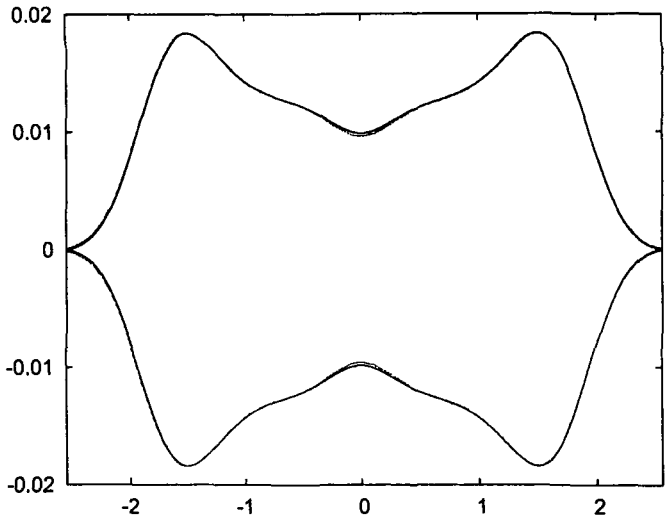

FIG. 6: Magnified theoretical and simulation hysteresis loops for $\sigma = 0.5$ where the magnetization along increasing and decreasing field is measured from the average of the magnetization on the lower and the upper half of the hysteresis loop in figure 5 at corresponding applied field.

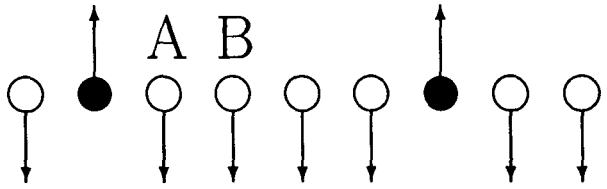

FIG. 7: Spins on Ramp-I in an applied field $-2|J| - h$. Filled circles show sites with quenched field $h_i > h$. The probability per site of a doublet (two adjacent down spins) such as AB is equal to e^{-2p}, where p is the fraction of filled circles on the infinite lattice.

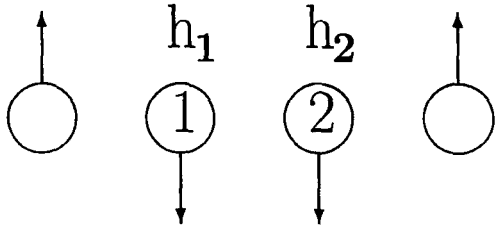

FIG. 8: A doublet on Plateau-I: h_1 and h_2 are the quenched random fields on the doublet sites 1 and 2 respectively.

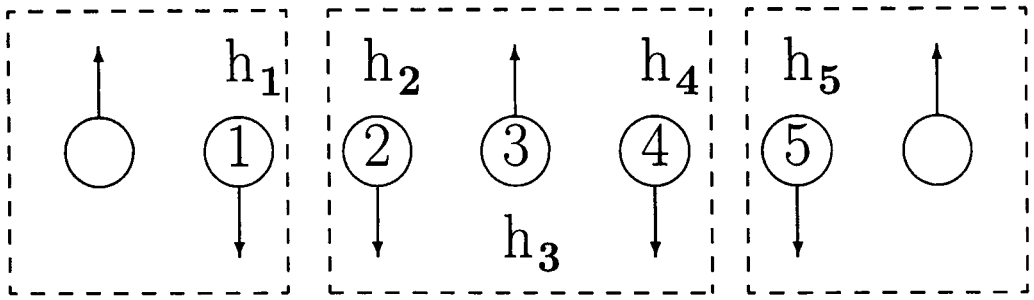

FIG. 9: Two adjacent doublets on Plateau-I: Each doublet separates the lattice into two parts whose evolution histories on Ramp-I are independent of each other. Evolutions inside each dashed box is shielded from outside. The probability that spin at site 3 flips up on Ramp-I is therefore equal to $\frac{1}{3}$. Given this, the probability that the spins at sites 1 and 5 remain down all along Ramp-I is equal to $\frac{1}{e}$ each. The shielding property of the boxes can also be used to determine a posteriori distribution of random fields h_1, h_2, h_3, h_4, and h_5.

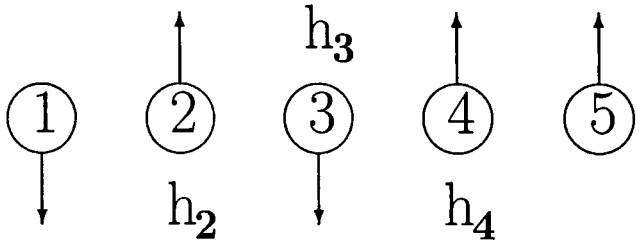

FIG. 10: A singlet (site 3) with one next nearest neighbor down (site 1), and one next nearest neighbor up (site 5). When the singlet turns up at an applied field h_a, the spin at site 2 stays up if $\Delta \leq |J|$, but the spin at site 4 flips down if $h_4 \leq h_3$.

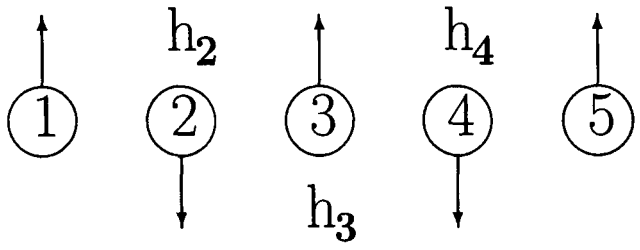

FIG. 11: Two adjacent singlets on Plateau-I: If $h_2 = \min(h_2, h_4)$, and $h_3 \leq h_2$, then the spin at site 3 will flip down when the spin at site 2 flips up on ramp-III. This process creates a new singlet on ramp-III.

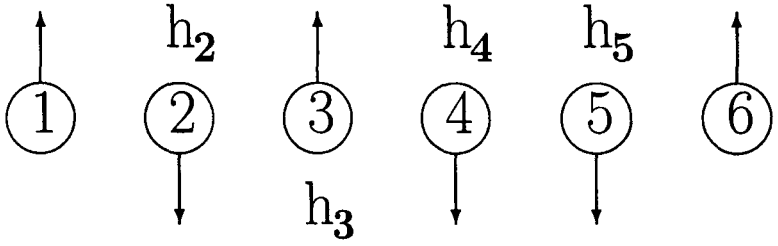

FIG. 12: A singlet followed by a doublet on Plateau-I: If $h_4 \geq h_5$, and $h_3 \leq h_2$, then a new singlet will be created at site 3 when the spin at site 2 turns up on ramp-III.

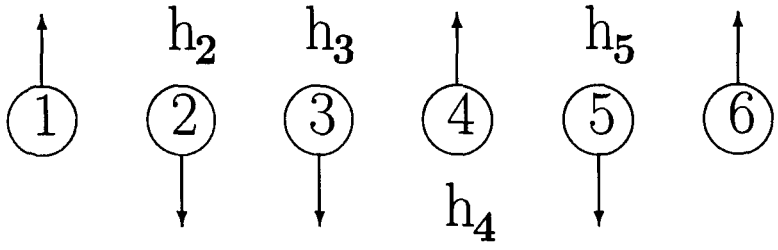

FIG. 13: A doublet followed by a singlet on Plateau-I: If $h_3 \geq h_2$, and $h_4 \leq h_5$, then a new singlet will be created at site 4 when the spin at site 5 turns up on ramp-III.

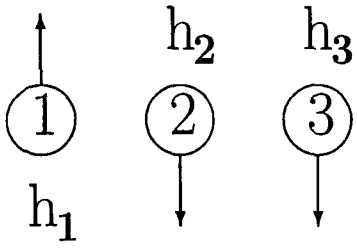

FIG. 14: An up spin followed by a doublet. Site-1 may have flipped up under a p_0-process or a p_1-process. Subsequently when site-3 flips up we get a singlet at site-2. The fraction of such singlets depends on the details of how sites 1 and 3 have flipped.

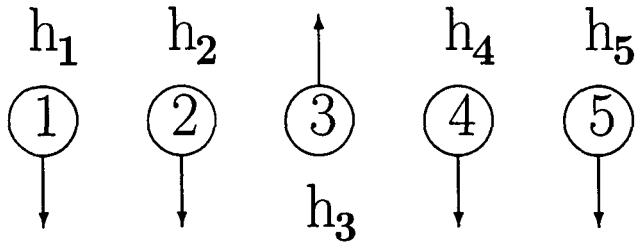

FIG. 15: A doublet followed by a doublet. We get a singlet at site-3 if sites 2 and 4 flip up before sites 1 and 5 and site-3 flips down because it is unstable with both neighbors up.

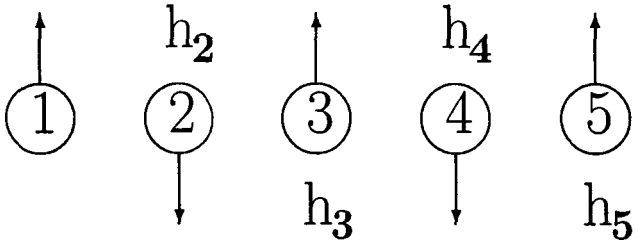

FIG. 16: A singlet followed by a singlet. A singlet is created at site-3 if sites 2 and 4 flip up under a p_2-process and then site-3 flips down because it is unstable when both neighbors are up.

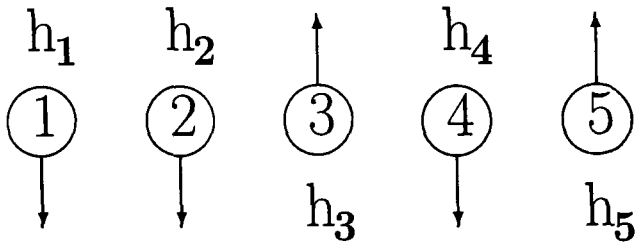

FIG. 17: A doublet followed by a singlet. We get a singlet at site-3 if site-2 flips up under a p_1-process, site-4 flips up under a p_2-process and then site-3 flips down because it is unstable when both neighbors are up.

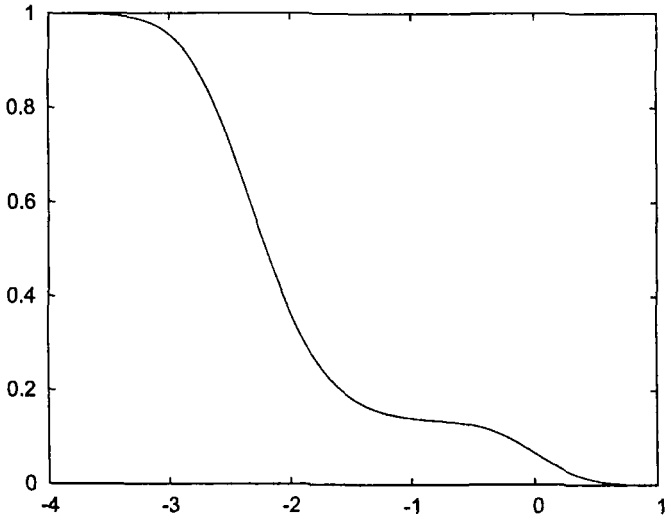

FIG. 18: Probability of a doublet $P_{\downarrow\downarrow}(h_a)$ for a Gaussian distribution with $\sigma = 0.5|J|$. Simulation data has been superimposed on the theoretical expression.

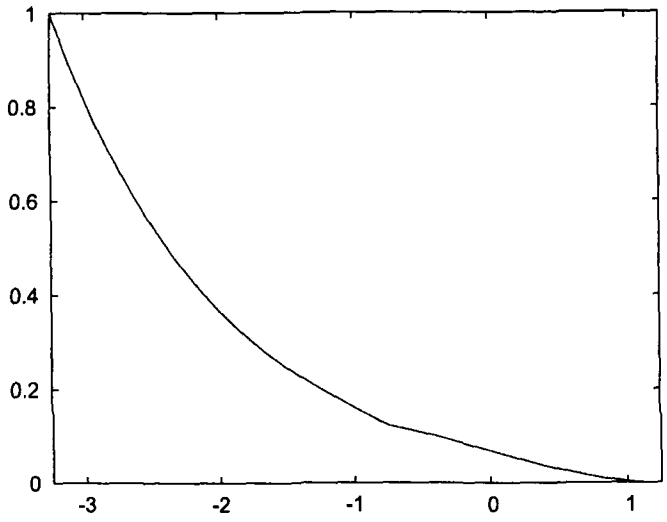

FIG. 19: Probability of a doublet $P_{\downarrow\downarrow}(h_a)$ for a uniform distribution with $\Delta = 1.25|J|$. Simulation data has been superimposed on the theoretical expression.

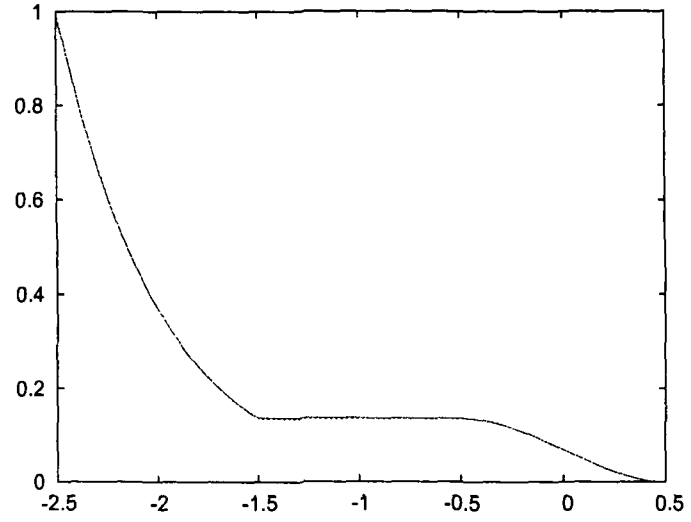

FIG. 20: Probability of a doublet $P_{\downarrow\downarrow}(h_a)$ for a uniform distribution with $\Delta = .5|J|$. Simulation data has been superimposed on the theoretical expression.

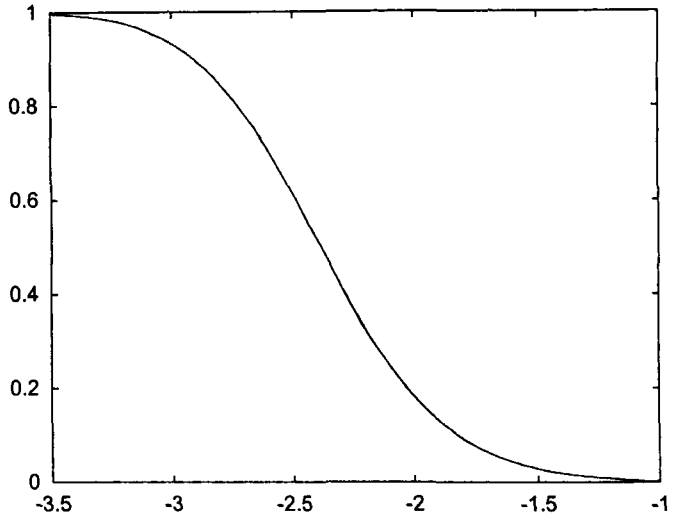

FIG. 21: Probability of $P_{\downarrow\downarrow\downarrow}(h_a)$ for a Gaussian distribution with $\sigma = 0.5|J|$. Simulation data has been superimposed on the theoretical expression.

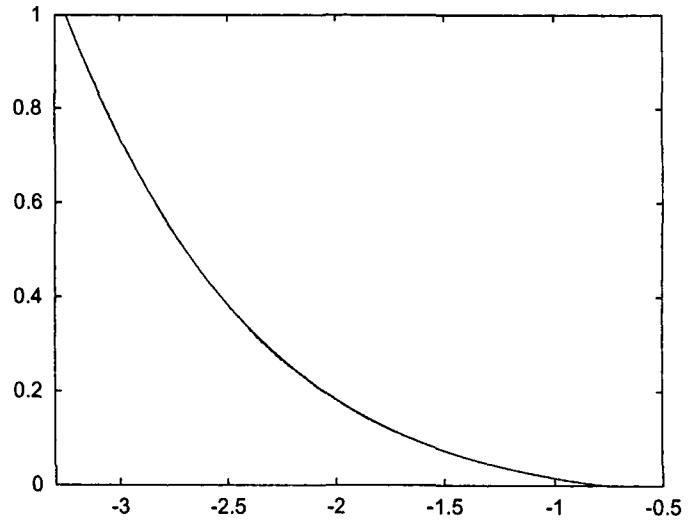

FIG. 22: Probability of $P_{\downarrow\downarrow\downarrow}(h_a)$ for a uniform distribution with $\Delta = 1.25|J|$. Simulation data has been superimposed on the theoretical expression.

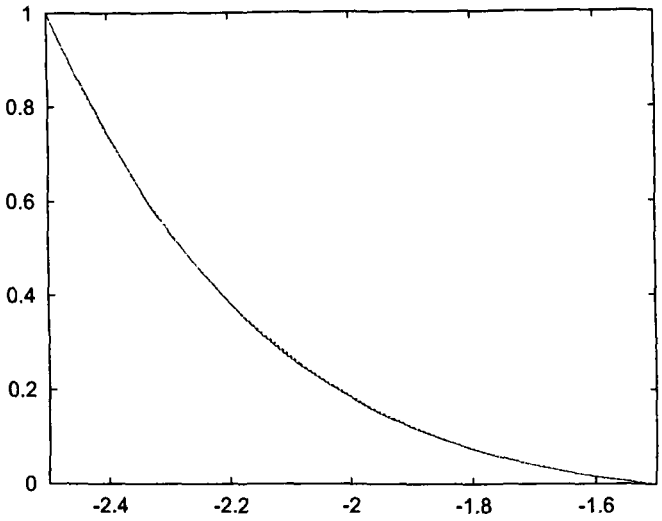

FIG. 23: Probability of $P_{\downarrow\downarrow\downarrow}(h_a)$ for a uniform distribution with $\Delta = 0.5|J|$. Simulation data has been superimposed on the theoretical expression.

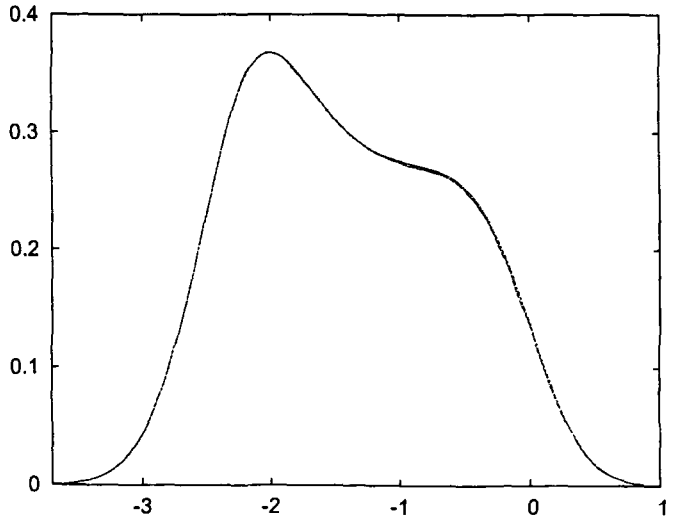

FIG. 24: $P_{\uparrow\downarrow\downarrow}(h_a) + P_{\downarrow\downarrow\uparrow}(h_a)$ for a Gaussian distribution with $\sigma = 0.5|J|$. Simulation data has been superimposed on the theoretical expression.

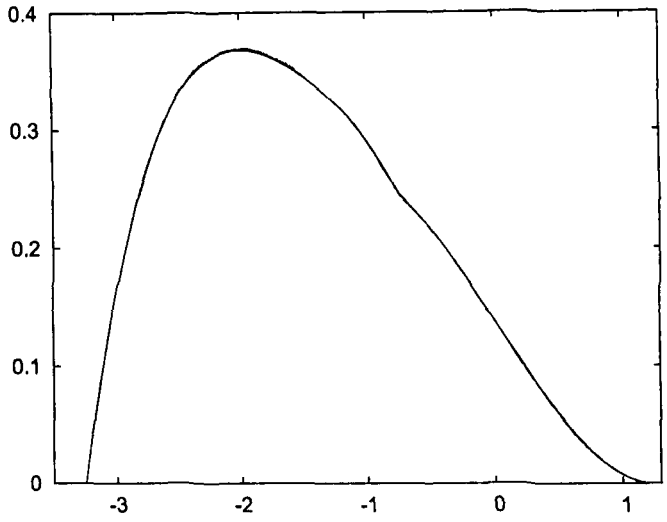

FIG. 25: $P_{\uparrow\downarrow\downarrow}(h_a) + P_{\downarrow\downarrow\uparrow}(h_a)$ for a uniform distribution with $\Delta = 1.25|J|$. Simulation data has been superimposed on the theoretical expression.

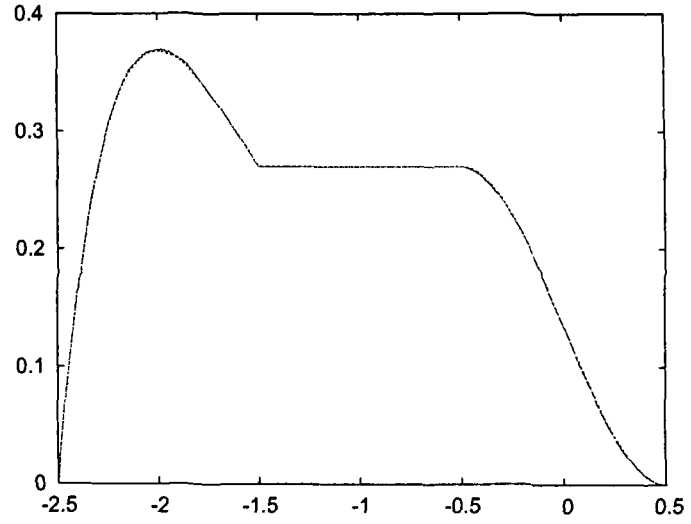

FIG. 26: $P_{\uparrow\downarrow\downarrow}(h_a) + P_{\downarrow\downarrow\uparrow}(h_a)$ for a uniform distribution with $\Delta = 0.5|J|$. Simulation data has been superimposed on the theoretical expression.

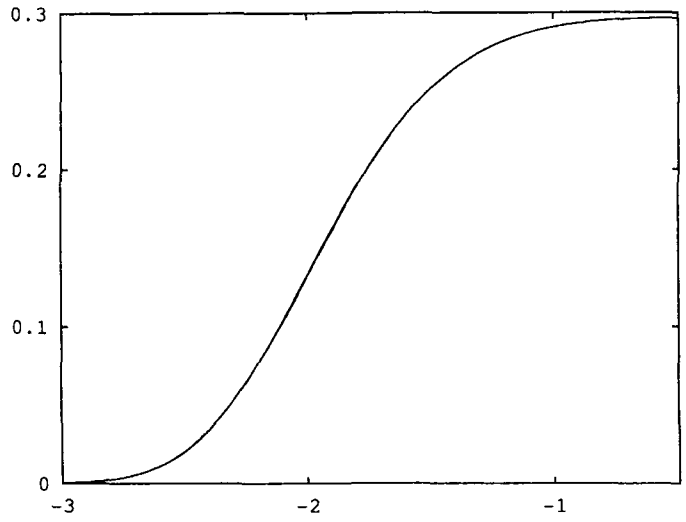

FIG. 27: Theory and simulation for $P_{\uparrow\downarrow\uparrow A}(h_a)$ for a Gaussian distribution with $\sigma = 0.5|J|$.

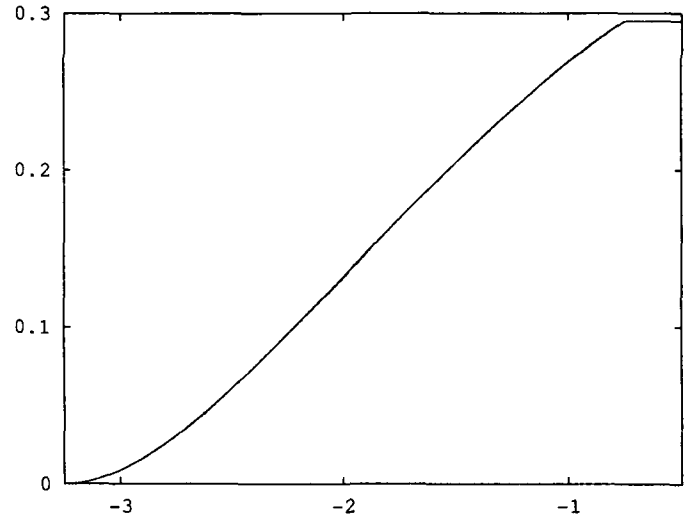

FIG. 28: Theory and simulation for $P_{\uparrow\downarrow\uparrow A}(h_a)$ for a uniform distribution with $\Delta = 1.25|J|$.

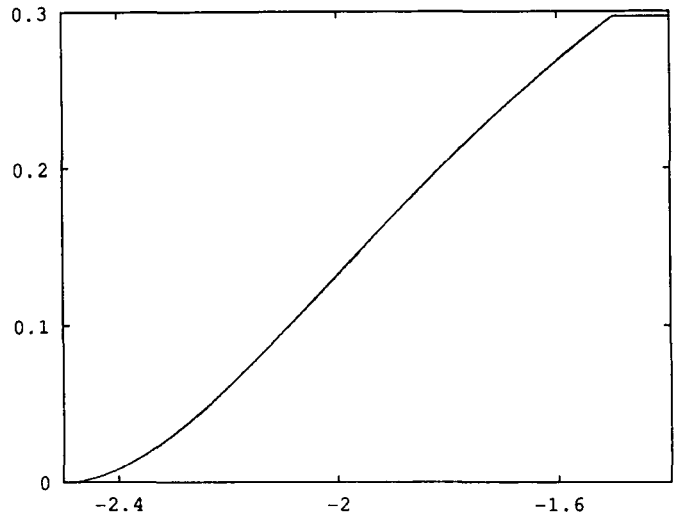

FIG. 29: Theory and simulation for $P_{\uparrow\downarrow\uparrow A}(h_a)$ for a uniform distribution with $\Delta = 0.5|J|$.

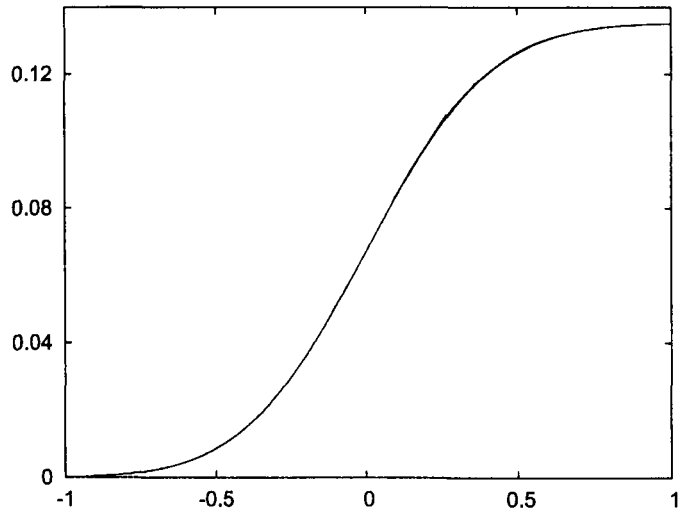

FIG. 30: Theory and simulation for $P_{\uparrow\downarrow\uparrow D}(h_a)$ for a Gaussian distribution with $\sigma = 0.5|J|$.

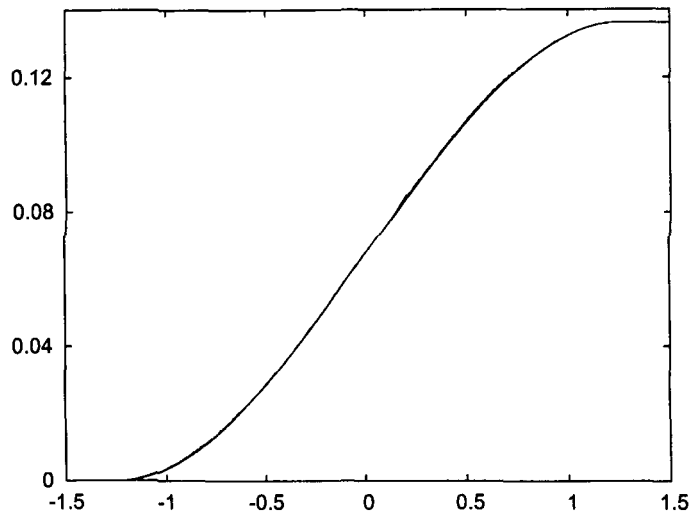

FIG. 31: Theory and simulation for $P_{\uparrow\downarrow\uparrow D}(h_a)$ for a uniform distribution with $\Delta = 1.25|J|$.

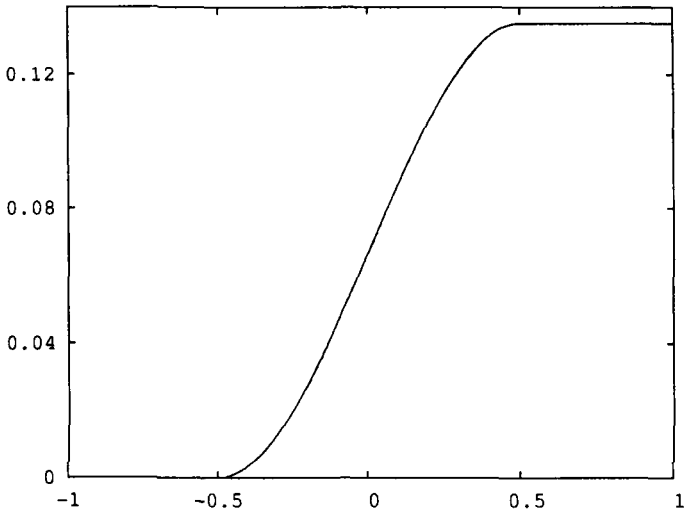

FIG. 32: Theory and simulation for $P_{\uparrow\downarrow\uparrow D}(h_a)$ for a uniform distribution with $\Delta = 0.5|J|$.

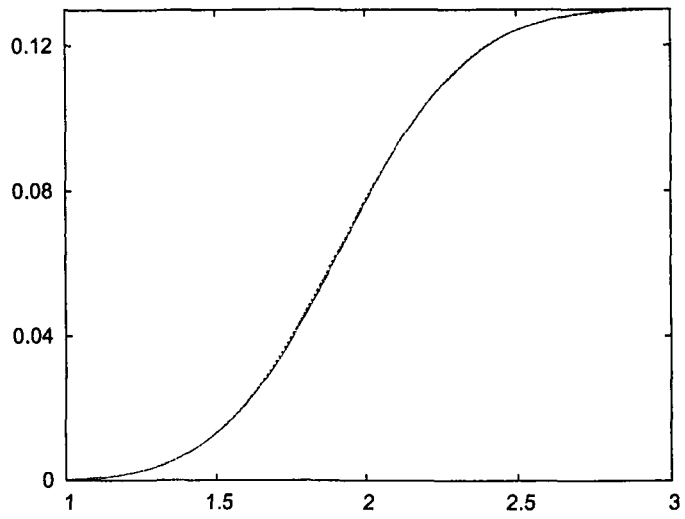

FIG. 33: Theory and simulation for $P_{\uparrow\uparrow\uparrow M}(h_a)$ for a Gaussian distribution with $\sigma = 0.5|J|$.

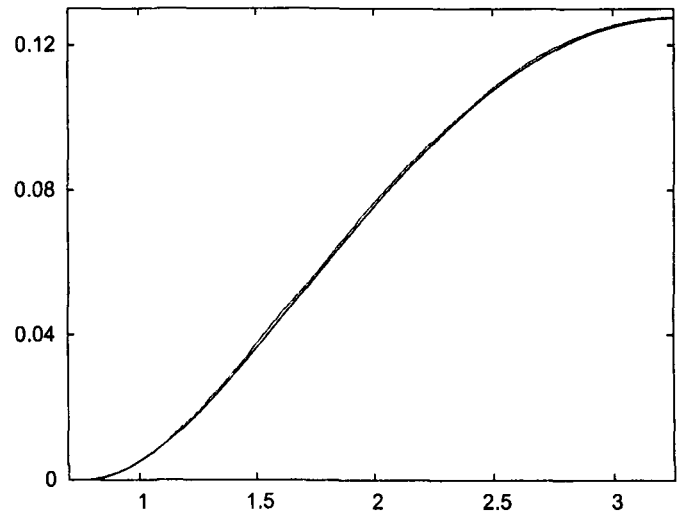

FIG. 34: Theory and simulation for $P_{\uparrow\uparrow\uparrow M}(h_a)$ for a uniform distribution with $\Delta = 1.25|J|$.

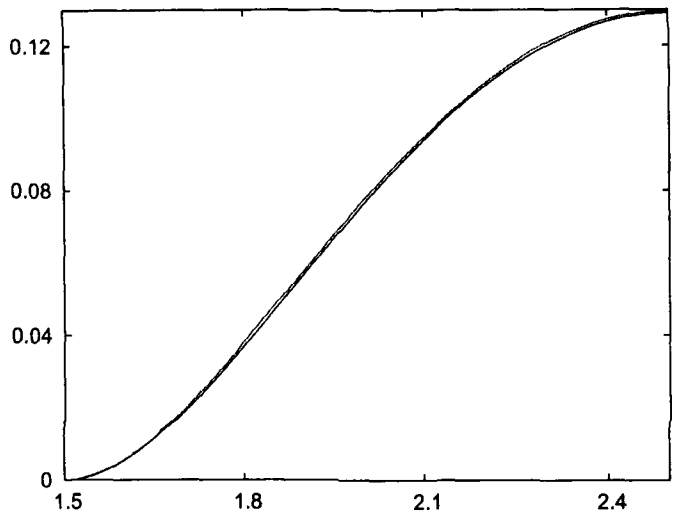

FIG. 35: Theory and simulation for $P_{\uparrow\uparrow\uparrow M}(h_a)$ for a uniform distribution with $\Delta = 0.5|J|$.

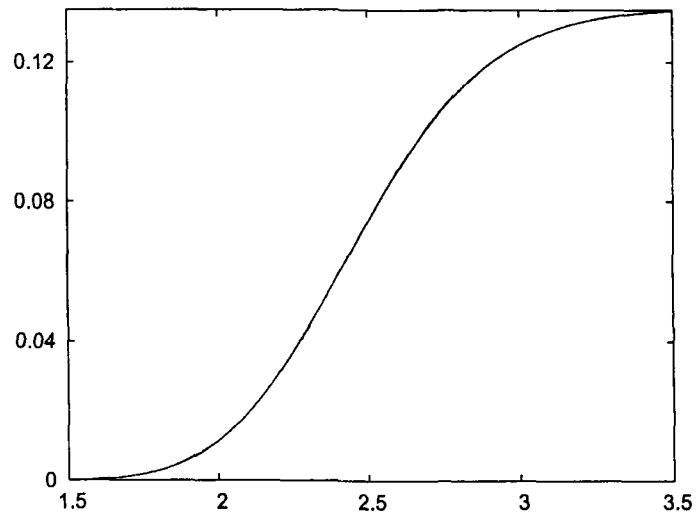

FIG. 36: Theory and simulation for $P_{\uparrow\uparrow\uparrow N}(h_a)$ for a Gaussian distribution with $\sigma = 0.5|J|$.

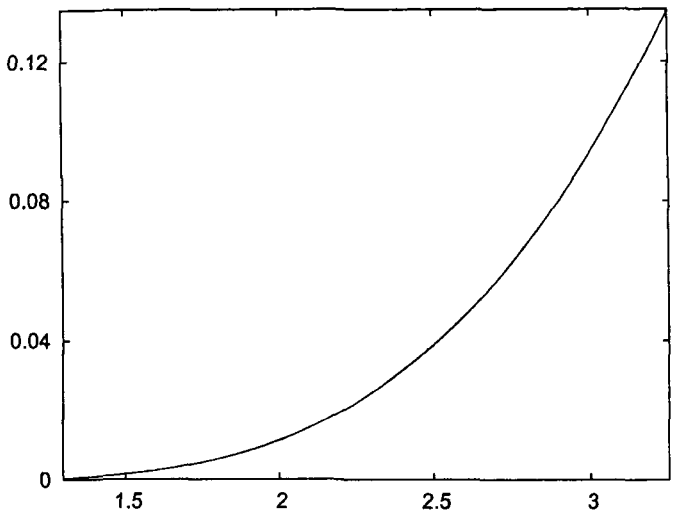

FIG. 37: Theory and simulation for $P_{\uparrow\uparrow\uparrow N}(h_a)$ for a uniform distribution with $\Delta = 1.25|J|$.

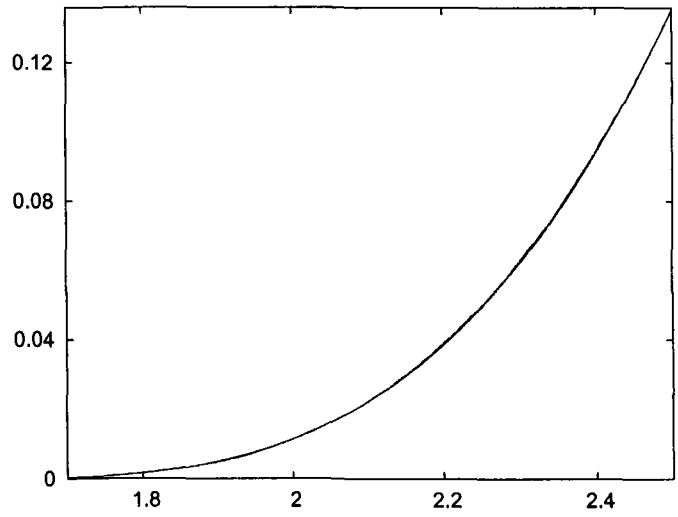

FIG. 38: Theory and simulation for $P_{\uparrow\uparrow\uparrow N}(h_a)$ for a uniform distribution with $\Delta = 0.5|J|$.

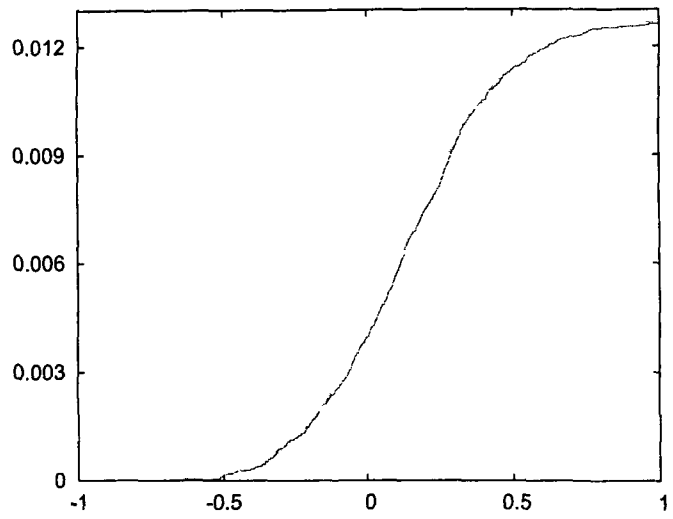

FIG. 39: Theory and simulation for $P_{\uparrow\downarrow\uparrow Q}(h_a)$ for a Gaussian distribution with $\sigma = 0.5|J|$.

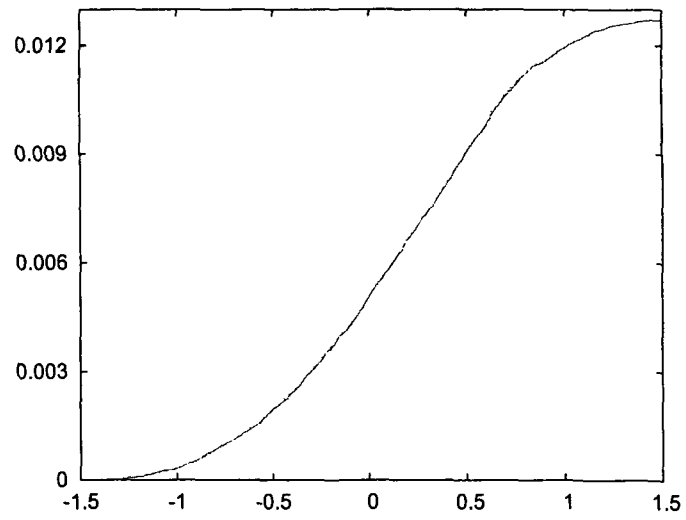

FIG. 40: Theory and simulation for $P_{\uparrow\downarrow\uparrow Q}(h_a)$ for a uniform distribution with $\Delta = 1.25|J|$.

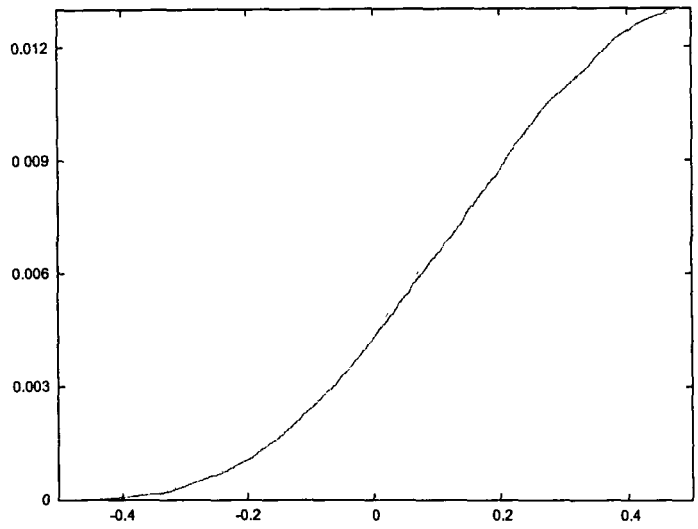

FIG. 41: Theory and simulation for $P_{\uparrow\downarrow\uparrow Q}(h_a)$ for a uniform distribution with $\Delta = 0.5|J|$.

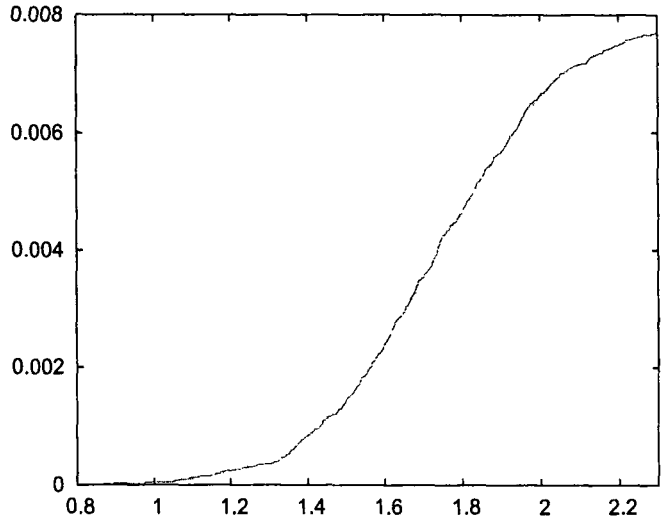

FIG. 42: Theory and simulation for $P_{\uparrow\uparrow\uparrow U}(h_a)$ for a Gaussian distribution with $\sigma = 0.5|J|$.

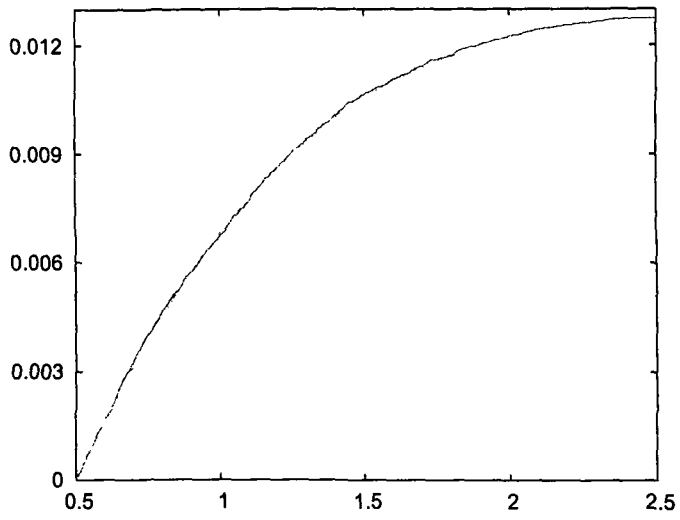

FIG. 43: Theory and simulation for $P_{\uparrow\uparrow\uparrow U}(h_a)$ for a uniform distribution with $\Delta = 1.25|J|$.

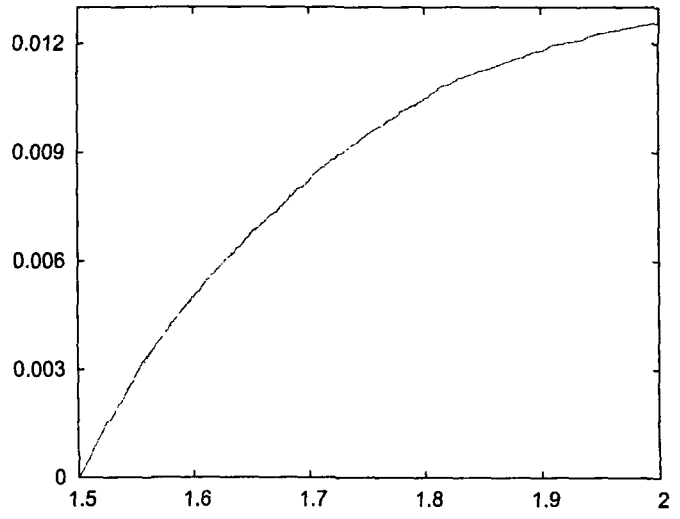

FIG. 44: Theory and simulation for $P_{\uparrow\uparrow\uparrow U}(h_a)$ for a uniform distribution with $\Delta = 0.5|J|$.

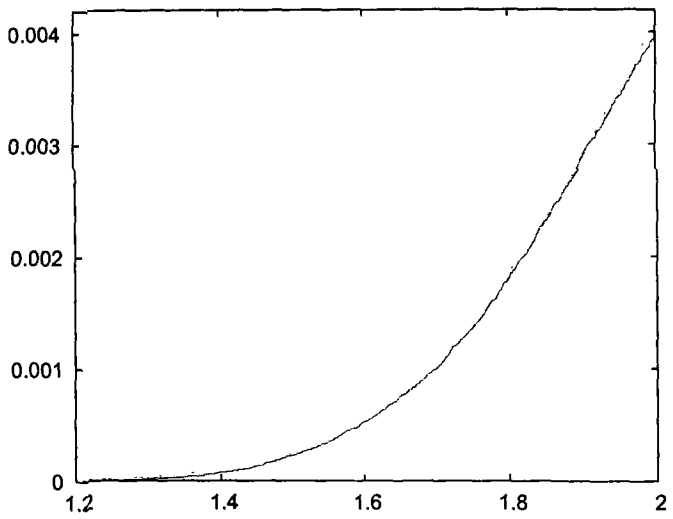

FIG. 45: Theory and simulation for $P_{\uparrow\uparrow\uparrow W}(h_a)$ on the left, and $P_{\uparrow\uparrow\uparrow W}(h_a)$ on the right for a Gaussian distribution with $\sigma = 0.5|J|$.

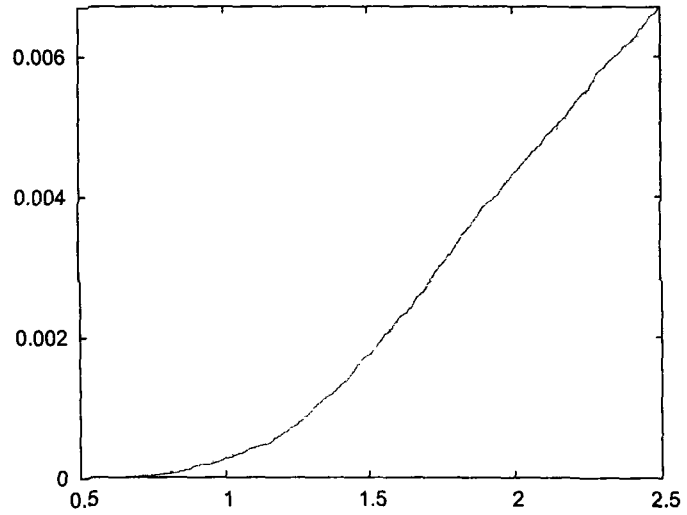

FIG. 46: Theory and simulation for $P_{\uparrow\uparrow\uparrow W}(h_a)$ for a uniform distribution with $\Delta = 1.25|J|$.

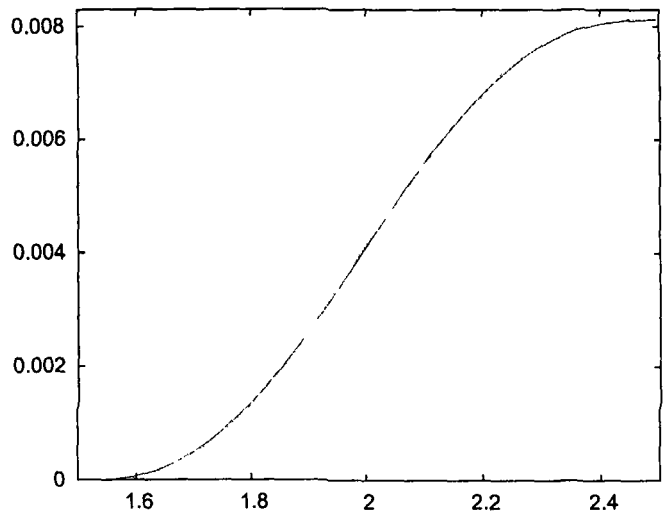

FIG. 47: Theory and simulation for $P_{\uparrow\uparrow\uparrow W}(h_a)$ for a uniform distribution with $\Delta = 0.5|J|$.

Brief Bio-data of the Candidate

(as required by NEHU format for PhD thesis)

Lobisor Kurbah cell phone 9863046871
Department of Physics email: kurbah88@gmail.com
St. Edmund's College
Shillong-793 003
Meghalaya, India.
Date of Birth: May 22, 1976; Unmarried.

Education:

Exam.	Institution	Year	Div.
High School	St Anthony's School, Shillong	1993	2nd
Pre Univ	St Edmund's College, Shillong	1995	Ist
B.Sc.	St Edmund's College, Shillong	1998	Ist
M.Sc.	NEHU, Shillong	2000	Ist

Teaching Experience:

Teaching Physics at B.Sc. level in St Edmund's College, Shillong from April, 2001 till date.